

A Saddle Point Approach to Structured Low-rank Matrix Learning in Large-scale Applications

Pratik Jawanpuria*

Bamdev Mishra*

July 28, 2022

Abstract

We propose a novel optimization approach for learning a low-rank matrix which is also constrained to be in a given linear subspace. Low-rank constraints are regularly employed in applications such as recommender systems and multi-task learning. In addition, several system identification problems require a learning matrix with both low-rank and linear subspace constraints. We model the classical nuclear norm regularized formulation as an equivalent saddle point minimax problem. This decouples the low-rank and the linear subspace constraints onto separate factors. Motivated by large-scale problems, we reformulate the minimax problem via a rank constrained non-convex surrogate. This translates into an optimization problem on the Riemannian spectrahedron manifold. We exploit the Riemannian structure to propose efficient first- and second-order algorithms. The duality theory allows to compute the duality gap for a candidate solution and our approach easily accommodates popular non-smooth loss functions, e.g., the absolute-value loss. We effortlessly scale on the Netflix data set on both matrix completion and robust matrix completion problems, obtaining state-of-the-art generalization performance. Additionally, we demonstrate the efficacy of our approach in Hankel matrix learning and multi-task learning problems.

1 Introduction

We study the following problem for learning low-rank matrix with structural constraints:

$$\begin{aligned} \min_{\mathbf{W} \in \mathbb{R}^{d \times T}} \quad & \frac{1}{2} \|\mathbf{W}\|_*^2 + CL(\mathbf{W}) \\ \text{subject to} \quad & \mathbf{W} \in \mathcal{D}, \end{aligned} \tag{1}$$

where $\|\mathbf{W}\|_* = \text{trace}(\sqrt{\mathbf{W}\mathbf{W}^\top})$ is the trace norm regularizer (also known as the nuclear norm), $L : \mathbb{R}^{d \times T} \rightarrow \mathbb{R} : \mathbf{W} \mapsto L(\mathbf{W})$ is a convex function, \mathcal{D} is a given linear subspace, and $C > 0$ is the regularization parameter. The trace norm regularizer promotes low rank solutions since $\|\mathbf{W}\|_*$ is equal to the ℓ_1 -norm on the singular values of \mathbf{W} (Fazel et al., 2001). The constraint $\mathbf{W} \in \mathcal{D}$ enforces particular structures on \mathbf{W} . $L(\mathbf{W})$ is commonly referred to as the loss term in machine learning applications.

Low rank solutions are desired in several settings such as the matrix completion problem within recommender systems (Candès & Recht, 2009), dimensionality reduction in multivariate regression (Yuan et al., 2007), and shared feature subspace learning for multiple problems within the multi-task learning framework (Amit et al., 2007; Argyriou et al., 2008). In addition to the low-rank

*Core Machine Learning Team, Amazon.com, Bengaluru 560055, India (e-mail: jawanpur,bamdevm@amazon.com).

constraint, other structural constraints may exist, such as the entry-wise non-negative constraint in non-negative matrix completion (Kannan et al., 2014). Several linear dynamical system models require learning a low-rank Hankel matrix (Fazel et al., 2013; Markovsky & Usevich, 2013). Hankel matrix has the structural constraint that all its anti-diagonal entries are same. Fazel et al. (2013) propose first-order optimization techniques to solve various primal and dual reformulations of (1) with the Hankel structure constraint. On the other hand, Markovsky & Usevich (2013) impose an explicit low-rank constraint and employ variable projection method to learn a low-rank matrix Hankel matrix. In robust matrix completion (Candès & Plan, 2009) and robust PCA (Wright et al., 2009) problems, the matrix is learned as a superimposition of a low-rank matrix and a sparse matrix. The sparse structure is modeled effectively by choosing $L(\mathbf{W})$ as the absolute-value loss (also known as the ℓ_1 -loss) function (Cambier & Absil, 2016).

In this paper, we propose to solve (1) via an *equivalent convex saddle point minimax* formulation. Conceptually, the *inner* maximization problem models the application specific characteristic along with the $\mathbf{W} \in \mathcal{D}$ structural constraint while the *outer* minimization problem enforces the low-rank constraint. The proposed approach enjoys several benefits. *First*, using the convex duality theory, the optimal solution of (1) is shown to be the product of two factors – one enforcing the trace norm constraint and the other enforcing the structural constraint ($\mathbf{W} \in \mathcal{D}$). Separating the low-rank and structural constraints onto different factors makes the optimization methodology much simpler, versatile, and scalable. The duality theory also helps to derive a duality gap convergence criterion for our algorithms, which can be computed efficiently. *Second*, the separability of the constraints allows replacing the trace norm constrained factor with a *rank restricted* surrogate. This is proposed to reduce the computational cost, thereby allowing us to scale to large-scale applications where low rank solutions are desired. Although this leads to a non-convex formulation, we provide a sufficient criterion of global optimality of our solution with respect to problem (1). In particular, following (Burer & Monteiro, 2003; Journée et al., 2010), we prove that if we obtain a rank-deficient local optimum for the proposed non-convex problem, we obtain the global optimum for problem (1). *Third*, we can easily employ general convex loss functions including non-smooth ones like the absolute-value loss or the hinge loss. In particular, we show experiments with the absolute-value loss on the Netflix data set. *Fourth*, the proposed approach allows us to exploit the scenarios where $d \ll T$ (or $T \ll d$) to drastically reduce the size of search space in, *e.g.*, matrix completion problems (Boumal & Absil, 2015). *Finally*, the proposed approach results in embarrassingly parallel inner maximization problems for several large-scale applications.

The proposed saddle point approach leads to an optimization problem on the Riemannian spectrahedron manifold (Journée et al., 2010). We exploit the Riemannian framework to propose computationally efficient conjugate gradient (first-order) and trust-region (second-order) algorithms.

Our contributions are as follows: (a) we propose a novel saddle point framework to learn structured low-rank matrix with generic convex loss functions; (b) we propose computationally efficient first- and second-order algorithms for our framework; (c) we provide the duality gap criterion as well as sufficient condition for global optimality; and (d) our algorithms achieve better generalization performance compared to state-of-the-art across various applications and easily scale to the Netflix data set for both standard and robust matrix completion problems.

The outline of the paper is as follows. We present our modeling of problem (1) in Section 2. The proposed optimization methodology is described in Section 3. In Section 4, we discuss the empirical results.

All the proofs are provided in the supplementary material. The Matlab codes are available at <https://bamdevmishra.com/codes/structuredmatrixlearning>.

2 Structured Low-rank Matrix Learning

We present our formulations and derivations for the generic multi-task learning setup. Specialized formulations for different applications are discussed in Section 2.3.

We begin by defining a few notations. Let T denotes the number of tasks (classification or regression problems) and let d be the dimension of the input feature space. Each task t has m_t training instances $\mathbf{X}_t \in \mathbb{R}^{d \times m_t}$ and corresponding labels $y_t \in \mathbb{R}^{m_t}$, where $\mathbf{X}_t = [x_{t1}, \dots, x_{tm_t}]$. The i^{th} instance-label pair for task t is $\{x_{ti}, y_{ti}\}$. For task t , the parameter vector is denoted by $w_t (\in \mathbb{R}^d)$ and the prediction function is $f_t(x) = w_t^\top x$. Let \mathbf{W} be a matrix with columns being $(w_t)_{t=1}^T$, i.e., $\mathbf{W} = [w_1, \dots, w_T]$. The loss term $L(\mathbf{W})$ in (1) is defined as $L(\mathbf{W}) := \sum_{t=1}^T \sum_{i=1}^{m_t} l(y_{ti}, w_t^\top x_{ti})$, where $l : \mathbb{R} \times \mathbb{R} \rightarrow \mathbb{R}$ is a convex loss function (convex in the second argument). The linear¹ subspace \mathcal{D} in problem (1) is represented as $\mathcal{D} := \{\mathbf{W} : \mathcal{A}(\mathbf{W}) = \mathbf{0}\}$, where $\mathcal{A} : \mathbb{R}^{d \times T} \rightarrow \mathbb{R}^n$ is a linear map and $\mathbf{0}$ is the null vector in \mathbb{R}^n . The set of $d \times d$ positive semi-definite matrices with unit trace is denoted by \mathcal{P}^d . The pseudoinverse of a matrix Θ is represented as Θ^\dagger .

Formulation (1) without the constraint $\mathbf{W} \in \mathcal{D}$ has been studied for multi-task feature learning application (Amit et al., 2007; Argyriou et al., 2008). The aim there is to learn a low dimensional latent subspace shared by all the tasks. However (1) is *non-smooth* and hence difficult to optimize directly. In this regard, we note the following *variational* characterization of the trace norm regularization (1).

Lemma 1. *Problem (1), with loss function L and set $\mathcal{D} := \{\mathbf{W} : \mathcal{A}(\mathbf{W}) = \mathbf{0}\}$, is equivalent to the problem*

$$\min_{\Theta \in \mathcal{P}^d} \sum_{t=1}^T \min_{w_t \in \mathbb{R}^d} \frac{1}{2} w_t^\top \Theta^\dagger w_t + C \sum_{i=1}^{m_t} l(y_{ti}, w_t^\top x_{ti}) \quad (2)$$

subject to $w_t \in \text{range}(\Theta) \forall t = 1, \dots, T$ and $\mathcal{A}(\mathbf{W}) = \mathbf{0}$, where $\text{range}(\Theta) = \{\Theta z : z \in \mathbb{R}^d\}$. For a given \mathbf{W} matrix, the optimal $\Theta^ = \sqrt{\mathbf{W}\mathbf{W}^\top} / \text{trace}(\sqrt{\mathbf{W}\mathbf{W}^\top})$.*

Proof. This result follows from Theorem 4.1 of Argyriou et al. (2006). □

The above lemma introduces a (feature) covariance matrix Θ and *transfers* the low-rank constraint over \mathbf{W} to Θ . The ranks of \mathbf{W} and Θ are equal at optimality. Hence, learning a low-rank Θ guarantees a low-rank \mathbf{W} as well. Existing works, which employ Lemma 1 for solving trace norm regularized problems, solve (2) via an alternate minimization procedure (Argyriou et al., 2008; Zhang & Yeung, 2010; Ciliberto et al., 2015). They require the eigenvalue decomposition of Θ at every alternate step, which is computationally costly for large-scale applications such as matrix completion on the Netflix data set. It should be noted that these works do not study additional structural constraints on \mathbf{W} .

Instead of directly optimizing problem (2), we study its dual formulation. In the next lemma, we derive the dual formulation of (2) with respect to \mathbf{W} .

Lemma 2. *Let l_{ti}^* be the Fenchel conjugate function of the loss: $l_{ti} : \mathbb{R} \rightarrow \mathbb{R}$, $v \mapsto l(y_{ti}, v)$. The dual problem of (2) with respect to \mathbf{W} is*

$$\min_{\Theta \in \mathcal{P}^d} g(\Theta), \quad (3)$$

¹A more generic form of \mathcal{D} is permissible within our framework: $\mathcal{D} := \{\mathbf{W} : \mathcal{A}_1(\mathbf{W}) = b_1, \mathcal{A}_2(\mathbf{W}) \leq b_2\}$. Its discussion is avoided in order keep the notations simple.

Optimization over Θ

$$\underbrace{\min_{\Theta \in \mathcal{P}^d} \max_{s \in \mathbb{R}^n, z_t \in \mathbb{R}^{m_t} \forall t} \sum_{t=1}^T \left(-C \sum_{i=1}^{m_t} l_{ti}^* \left(\frac{-z_{ti}}{C} \right) - \frac{1}{2} (\mathbf{X}_t z_t + a_t)^\top \Theta (\mathbf{X}_t z_t + a_t) \right)}_{\text{Application specific algorithm}}$$

Application specific algorithm

Figure 1: The proposed optimization framework decouples low-rank and structural constraints onto separate factors. Low-rank learning is enforced by optimization over Θ , whereas the structural constraints are enforced with optimization over the dual variables $\{s, (z_t)_{t=1}^T\}$.

where $g : \mathcal{P}^d \rightarrow \mathbb{R} : \Theta \mapsto g(\Theta)$ is the following convex function

$$g(\Theta) := \max_{s \in \mathbb{R}^n} \sum_{t=1}^T \left(\max_{z_t \in \mathbb{R}^{m_t}} -C \sum_{i=1}^{m_t} l_{ti}^* \left(\frac{-z_{ti}}{C} \right) - \frac{1}{2} (\mathbf{X}_t z_t + a_t)^\top \Theta (\mathbf{X}_t z_t + a_t) \right). \quad (4)$$

Here, $a_t \in \mathbb{R}^d$ for $t = \{1, \dots, T\}$, where $[a_1, \dots, a_T] = \mathcal{A}^*(s)$ and $\mathcal{A}^* : \mathbb{R}^n \rightarrow \mathbb{R}^{d \times T}$ is the adjoint of \mathcal{A} .

Furthermore, let Θ^* be an optimal solution of (3) and $\{s^*, (z_t^*)_{t=1}^T\}$ be corresponding optimal solution of (4), then the optimal solution $\mathbf{W}^* := [w_1^*, \dots, w_T^*]$ of (2) is given by $w_t^* = \Theta^*(X_t z_t^* + a_t^*)$, where $[a_1^*, \dots, a_T^*] = \mathcal{A}^*(s^*)$.

Proof. The lemma follows from the Lagrangian duality. The proof is provided in the supplementary material. \square

Lemma 2 provides further insights into the problem. First, the optimal w_t^* is a product of two terms, Θ^* and $X_t z_t^* + a_t^*$. The low-rank constraint is enforced through Θ^* and the structural constraint is enforced through $X_t z_t^* + a_t^*$. This facilitates employing simpler optimization techniques as compared to the case where both the constraints are enforced on a single variable. In applications where the constraint $\mathcal{A}(\mathbf{W}) = \mathbf{0}$ is absent, the problem (4) can be solved in parallel across t , as single task learning problems. Several highly optimized publicly available solvers can be employed for single-task problems. It should be noted that the dual formulation (4) is smooth (with bounded constraints on the dual variables z) even for non-smooth loss functions such as the absolute-value loss. Figure 1 illustrates the overall optimization framework for (3), discussed in subsequent sections.

Depending on the regularization parameter C , the solution to (3) is approximately low rank. Putting a smaller value of C gives a lower-rank solution, but at a higher training loss. To circumvent this, we explicitly constrain the rank of Θ in (3). In fact, several works (Boumal & Absil, 2011; Cambier & Absil, 2016) have shown good generalization performance on the Netflix data set by explicitly constraining the rank of \mathbf{W} to as low as 10.

2.1 Fixed-rank Parameterization of Θ

We model $\Theta \in \mathcal{P}^d$ as a rank r matrix as follows: $\Theta = \mathbf{U}\mathbf{U}^\top$, where $\mathbf{U} \in \mathbb{R}^{d \times r}$ and $\|\mathbf{U}\|_F = 1$. The implications of the proposed modeling are discussed below.

First, the $\Theta \in \mathcal{P}^d$ constraint is always satisfied by the above parameterization. Hence, we avoid the computational cost of ensuring $\Theta \in \mathcal{P}^d$ at each step of the optimization algorithm. As

Table 1: Specialized expression of $g(\mathbf{U}\mathbf{U}^\top)$ as defined in (6), algorithm for computing it and the expression for recovering the primal variables w_t for various low rank structured matrix learning applications employing different loss functions.

Application	$l(y, w^\top x)$	$g(\mathbf{U}\mathbf{U}^\top)$ as defined in (6)	Computing $g(\mathbf{U}\mathbf{U}^\top)$	w_t
Matrix [‡] Completion	$(y - w^\top x)^2$	$\max_{z_t \in \mathbb{R}^{m_t} \forall t} \sum_{t=1}^T \langle y_t, z_t \rangle - \frac{1}{4C} \langle z_t, z_t \rangle - \frac{1}{2} \langle \mathbf{U}_{\Omega_t}^\top z_t, \mathbf{U}_{\Omega_t}^\top z_t \rangle$	Least square solver [§]	$\mathbf{U}_{\Omega_t} (\mathbf{U}_{\Omega_t}^\top z_t)$
Robust [‡] Matrix Completion	$ y - w^\top x $	$\max_{z_t \in [-C, C]^{m_t} \forall t} \sum_{t=1}^T \langle y_t, z_t \rangle - \frac{1}{2} \langle \mathbf{U}_{\Omega_t}^\top z_t, \mathbf{U}_{\Omega_t}^\top z_t \rangle$	Dual coordinate descent [§] (Ho & Lin, 2012)	$\mathbf{U}_{\Omega_t} (\mathbf{U}_{\Omega_t}^\top z_t)$
Non- negative [‡] Matrix Completion	$(y - w^\top x)^2$	$\max_{\substack{z_t \in \mathbb{R}^{m_t} \forall t, \\ s_t \in [0, \infty)^{m_t} \forall t}} \sum_{t=1}^T \langle y_t, z_t \rangle - \frac{1}{4C} \langle z_t, z_t \rangle - \frac{1}{2} \langle \mathbf{U}_{\Omega_t}^\top (z_t + s_t), \mathbf{U}_{\Omega_t}^\top (z_t + s_t) \rangle$	Dual coordinate descent [§] (Ho & Lin, 2012)	$\mathbf{U}_{\Omega_t} (\mathbf{U}_{\Omega_t}^\top (z_t + s_t))$
Hankel Matrix Learning	$(y - w^\top x)^2$	$\max_{\substack{z_t \in \mathbb{R}^{m_t} \forall t, z \in \mathbb{R}^{d+T-1} \\ \text{subject to } :z_k - \sum_{\substack{(i,t): i+t=k, \\ 1 \leq i \leq d, 1 \leq t \leq T}} s_{ti} = 0 \ \forall k = 2, \dots, d+T}}$	Preconditioned [#] conjugate gradients (Barrett et al., 1994)	$\mathbf{U}_{\Omega_t} (\mathbf{U}_{\Omega_t}^\top s_t)$

[‡] $\mathbf{U}_{\Omega_t} \in \mathbb{R}^{m_t \times r}$ represents a matrix with only those rows of \mathbf{U} whose corresponding indices are present in Ω_t .
[§] Parallelizable across the tasks. [#] The equality constraints are handled efficiently by using an affine projection operator.

discussed earlier, the existing works that learn a low rank Θ (Argyriou et al., 2008; Zhang & Yeung, 2010; Jawanpuria & Nath, 2011; Ciliberto et al., 2015) employ $O(d^3)$ computation (eigenvalue decomposition of a $d \times d$ matrix) for this purpose. Enforcing the constraint $\|\mathbf{U}\|_F = 1$, on the other hand, costs $O(rd)$. *Second*, the dimension of the search space of problem (3) with $\Theta = \mathbf{U}\mathbf{U}^\top$ is $rd - 1 - r(r-1)/2$ (Journée et al., 2010), which is much lower than the dimension $(d(d+1)/2 - 1)$ of $\Theta \in \mathcal{P}^d$. As noted earlier, $r \ll d$ is popularly employed in various large-scale applications. *Third*, the set of fixed-rank positive semi-definite matrices with unit trace has the structure of a smooth (quotient) manifold (Journée et al., 2010). This allows us to propose highly efficient first- and second-order algorithms for (3).

Although $g(\mathbf{U}\mathbf{U}^\top)$ is a non-convex function in \mathbf{U} , we provide sufficient condition for global optimality with respect to (3) in the next section. We also provide a duality gap expression for any feasible solution $\hat{\Theta} = \hat{\mathbf{U}}\hat{\mathbf{U}}^\top$ of (3).

2.2 Sufficient Condition for Global Optimality

We first re-write (3) and (4) in terms of the proposed parameterization $\Theta = \mathbf{U}\mathbf{U}^\top$, which is as follows:

$$\min_{\mathbf{U} \in \mathbb{R}^{d \times r}} g(\mathbf{U}\mathbf{U}^\top), \text{ subject to } \|\mathbf{U}\|_F = 1, \quad (5)$$

where the function $g(\mathbf{U}\mathbf{U}^\top)$ is defined as follows, *i.e.*,

$$g(\mathbf{U}\mathbf{U}^\top) := \max_{s \in \mathbb{R}^n} \sum_{t=1}^T \max_{z_t \in \mathbb{R}^{m_t}} \left(-C \sum_{i=1}^{m_t} l_{ti}^* \left(\frac{-z_{ti}}{C} \right) - \frac{1}{2} \left\| \mathbf{U}^\top (X_t z_t + a_t) \right\|_F^2 \right). \quad (6)$$

We emphasize that though (5) is a non-convex problem in \mathbf{U} , the optimization problem in (6) is convex in $\{s, (z_t)_{t=1}^T\}$ for a given \mathbf{U} . The following lemma provides a characterization of an optimal solution of the convex problem (3).

Lemma 3. Let \mathbf{U}^* be a local minimizer of the non-convex problem (5). If $\text{rank}(\mathbf{U}^*) < r$ or $r = d$, then $\Theta^* = \mathbf{U}^*(\mathbf{U}^*)^\top$ is a stationary point for the convex problem (3).

Proof. The above result is a special case of the general result proved by Journée et al. (2010, Theorem 7 and Corollary 8). \square

Consequently, given a local minimizer \mathbf{U}^* of (5), we can verify whether the candidate solution $\Theta = \mathbf{U}^*(\mathbf{U}^*)^\top$ is optimal for (3) by simply computing the minimum singular value of \mathbf{U}^* . Computing the minimum singular value costs $O(dr^2)$, which is computationally efficient for $r \ll d$.

Lemma 3, however, requires computing a local minimizer of (5) in order to check global optimality for (3). Our next result provides a duality gap certificate for (3) with respect to any feasible solution $\hat{\mathbf{U}}$ of (5).

Proposition 1. Let $\hat{\mathbf{U}}$ be a feasible solution for the problem (5). Then, a candidate solution for (3) is $\hat{\Theta} = \hat{\mathbf{U}}\hat{\mathbf{U}}^\top$. Let $\{\hat{s}, (\hat{z}_t)_{t=1}^T\}$ be an optimal solution of the convex problem in (6) corresponding to $\hat{\mathbf{U}}$. In addition, let σ_1 be the maximum singular of the matrix whose t^{th} column is $(X_t\hat{z}_t + \hat{a}_t)$, where $[\hat{a}_1, \dots, \hat{a}_T] = \mathcal{A}^*(\hat{s})$. The duality gap (Δ) associated with $\{\hat{\Theta}, \hat{s}, (\hat{z}_t)_{t=1}^T\}$ for problem (3) is given by

$$\Delta = \frac{1}{2} \left(\sigma_1^2 - \sum_{t=1}^T \left\| \hat{\mathbf{U}}^\top (X_t\hat{z}_t + \hat{a}_t) \right\|^2 \right). \quad (7)$$

Proof. The proof follows from min-max interchange (Sion, 1958) in problem (3) and the result that the spectral norm is the dual norm of the trace norm (Boyd & Vandenberghe, 2004). Complete proof is in the supplementary material. \square

Computation of Δ for the general case costs $O(dTr + d\sum_t m_t)$, given $(\hat{a}_t)_{t=1}^T$. However, applications with specialized formulations may have much lower computational complexity for Δ . For example, in the matrix completion problem, where $r \ll d$, its computational cost is only linear with the number of known entries. We present such specialized formulations for a wide range of applications in the next section.

2.3 Specialized Formulations for Various Applications

Problems (5) and (6) can easily be specialized to various other applications as discussed below.

Matrix completion: Given a partially observed matrix \mathbf{Y} at indices Ω , we learn the full matrix \mathbf{W} (Cai et al., 2010; Toh & Yun, 2010).

Robust matrix completion: Matrix completion with robust loss function such as the absolute-value loss function (Candès & Plan, 2009; Cambier & Absil, 2016).

Robust PCA: Similar to robust matrix completion, but with all the entries observed (Candès et al., 2011).

Non-negative matrix completion: Matrix completion with the constraint that each entry is non-negative.

Hankel Matrix Learning: Hankel matrices have the structural constraint that its anti-diagonal entries are same. Given a vector $y = [y_1, y_2, \dots, y_7]$, a Hankel matrix corresponding to it is

$$\begin{bmatrix} y_1 & y_2 & y_3 & y_4 & y_5 \\ y_2 & y_3 & y_4 & y_5 & y_6 \\ y_3 & y_4 & y_5 & y_6 & y_7 \end{bmatrix}. \quad (8)$$

In certain linear time-invariant systems, learning a low-rank Hankel matrix corresponding to a given vector y is equivalent to finding a low-complexity linear model for the data (Fazel et al., 2013; Markovsky & Usvich, 2013; Markovsky, 2014).

The above applications have the following common problem setup: we need to learn \mathbf{W} *similar* to a given (partially observed) matrix \mathbf{Y} . Let Ω_t (Ω) be the set of observed entries for w_t (\mathbf{W}) and let $m_t = |\Omega_t|$. The loss function in such settings is a function of only \mathbf{W} and \mathbf{Y} . However, in accordance with the multi-task learning notations, the loss for each of the considered applications is re-written as $L(\mathbf{W}) = \sum_{t=1}^T \sum_{i \in \Omega_t} l(y_{ti}, w_t^\top x_{ti})$, where $x_{ti} \in \mathbb{R}^d$, $x_{ti}(j) = 1$ if $j = i$, and 0 otherwise. By the above construction, $w_t^\top x_{ti} = w_{ti} \forall i \in \Omega_t$.

Table 1 lists the expressions of $g(\mathbf{U}\mathbf{U}^\top)$ as defined in (6) for such applications. We discuss empirical results on these applications as well as on multi-task learning in Section 4. In the next section, we present our optimization algorithm to obtain a local minima of problem (5).

3 Optimization over Spectrahedron Manifold

One approach to optimize (5) is by employing the standard (Euclidean) projected gradient descent and Newton techniques (Bertsekas, 1999, Chapter 2). This requires the computation of the gradient $\nabla_{\mathbf{U}} g(\mathbf{U}\mathbf{U}^\top)$ and an orthogonal projection onto the unit sphere of dimension $dr - 1$.

A more direct approach exploits the fact that the matrix \mathbf{U} lies in, what is popularly known as, the *spectrahedron* manifold $\mathcal{S}_r^d := \{\mathbf{U} \in \mathbb{R}^{d \times r} : \|\mathbf{U}\|_F = 1\}$. Specifically, the spectrahedron manifold has the structure of a Riemannian (quotient) manifold (Journée et al., 2010), and hence, the problem (5) has the equivalent formulation

$$\min_{\mathbf{U} \in \mathcal{S}_r^d} g(\mathbf{U}\mathbf{U}^\top). \quad (9)$$

It should be noted that the problem (9) is conceptually different from (5) in the way that the constraint is now embedded into the search space. The benefit of the Riemannian manifold optimization framework is that it allows to translate the constrained optimization problem (5) into an *unconstrained* optimization problem over the nonlinear manifold \mathcal{S}_r^d . The conventional (Euclidean) first- (*e.g.*, steepest descent and conjugate gradients) and second-order (trust regions) algorithms have their Riemannian manifold counterparts with similar convergence guarantees (Absil et al., 2008; Journée et al., 2010).

Our framework is readily amenable to Riemannian conjugate gradient and trust-region algorithms (Absil et al., 2008; Sato & Iwai, 2013), which employ the notions of the *Riemannian gradient* (first-order derivative of the objective function on the manifold), *Riemannian Hessian* along a search direction (the *covariant* derivative of the Riemannian gradient along a tangential direction on the manifold), and the *retraction* operator (that ensures that we always stay on the manifold). Once these notions are defined, we can employ the publicly available toolboxes, *e.g.*, Manopt (Boumal et al., 2014), for an efficient implementation. The Riemannian gradient and Hessian notions require computations of the standard (Euclidean) gradient of the objective function and the directional derivative of this gradient along a given search direction (9). The following lemma shows the concrete matrix expressions of the gradient and its directional derivative.

Algorithm 1 Proposed algorithm for (5)

```
1: Input:  $\{X_t, y_t\}_{t=1}^T$ , rank  $r$ , parameter  $C$  and solver.
2: Output:  $\{\mathbf{U}, s, (z_t)_{t=1}^T\}$  ( $\mathbf{W}$  is computed from these using Lemma 2).
3: Initialize  $\mathbf{U}$ .
4: repeat
5:   Solve for  $\{s, (z_t)_{t=1}^T\}$  by computing  $g(\mathbf{U}\mathbf{U}^T)$  as defined in (6). Refer Table 1 for specialized problems.
6:   Compute  $\nabla g(\mathbf{U}\mathbf{U}^T)$  as in Lemma 4.
7:   if solver is 'Riemannian conjugate gradient' then
8:     /* Riemannian conjugate gradient step (first-order) */
9:     Compute a conjugate direction  $\mathbf{V}$  and the corresponding step size  $\alpha$ .
10:     $\mathbf{U} = (\mathbf{U} + \alpha\mathbf{V}) / \|\mathbf{U} + \alpha\mathbf{V}\|_F$  (retraction operator).
11:   else
12:     /* Riemannian trust-region step (second-order) */
13:     Compute a search direction  $\mathbf{V}$  which minimizes the trust region sub-problem. This makes use of the directional derivative  $D\nabla g(\mathbf{U}\mathbf{U}^T)[\mathbf{V}]$  as in Lemma 4.
14:      $\mathbf{U} = (\mathbf{U} + \mathbf{V}) / \|\mathbf{U} + \mathbf{V}\|_F$  (retraction operator).
15:   end if
16: until convergence
```

Lemma 4. Let $\{s, (z_t)_{t=1}^T\}$ be an optimal solution of the convex problem (6) at \mathbf{U} . Then,

$$\begin{aligned}\nabla g(\mathbf{U}\mathbf{U}^T) &= -\left(\sum_{t=1}^T (X_t z_t + a_t)(X_t z_t + a_t)^\top\right)\mathbf{U} \\ D\nabla g(\mathbf{U}\mathbf{U}^T)[\mathbf{V}] &= -\left(\sum_{t=1}^T (X_t z_t + a_t)(X_t z_t + a_t)^\top\right)\mathbf{V} \\ &\quad -\left(\sum_{t=1}^T (X_t \dot{z}_t + \dot{a}_t)(X_t z_t + a_t)^\top\right)\mathbf{U} \\ &\quad -\left(\sum_{t=1}^T (X_t z_t + a_t)(X_t \dot{z}_t + \dot{a}_t)^\top\right)\mathbf{U},\end{aligned}$$

where $\nabla g(\mathbf{U}\mathbf{U}^T)$ is the gradient of $g(\mathbf{U}\mathbf{U}^T)$ at \mathbf{U} , $D\nabla g(\mathbf{U}\mathbf{U}^T)[\mathbf{V}]$ is the directional derivative of the gradient $\nabla g(\mathbf{U}\mathbf{U}^T)$ along $\mathbf{V} \in \mathbb{R}^{d \times r}$. Here, $\{\dot{s}, (\dot{z}_t)_{t=1}^T\}$ is directional derivative of $\{s, (z_t)_{t=1}^T\}$ along \mathbf{V} and at optimality of the convex problem (6) for the given \mathbf{U} .

Proof. The gradient is computed by employing the Danskin's theorem (Bertsekas, 1999; Bonnans & Shapiro, 2000). The directional derivative of the gradient follows directly from the chain rule. \square

At every iteration, the Riemannian nonlinear conjugate gradient algorithm computes a *conjugate* direction. We perform *Armijo* linesearch on the manifold to compute a step-size that sufficiently decreases the objective function. Once a step-size computed, we update along the conjugate direction with the step-size.

The Riemannian trust-region algorithm solves a trust-region *sub-problem* (in a neighborhood) at every iteration. Solving the trust-region sub-problem leads to a search direction that minimizes a quadratic model of the objective function on the manifold. Practically, solving this sub-problem does not require inverting the full Hessian of the objective function. Instead there exists iterative algorithms that make use of the directional derivative of the gradient (as computed in Lemma 4). Once a search direction is computed, a potential update along it (with the retraction operator) is accepted only when the decrease of the objective function is sufficient (Absil et al., 2008, Chapter 7).

Algorithm 1 summarizes the proposed algorithms for solving (5).

Although we have focused on batch algorithms in this section, our framework can be extended to stochastic settings, *e.g.*, when the tasks are streamed one by one. In this case, when a new task is received, we perform a (stochastic) gradient update on \mathcal{S}_r^d . Convergence analysis of stochastic gradients (and their variants) algorithms have been discussed in the recent works (Bonnabel, 2013; Zhang et al., 2016; Sato et al., 2017).

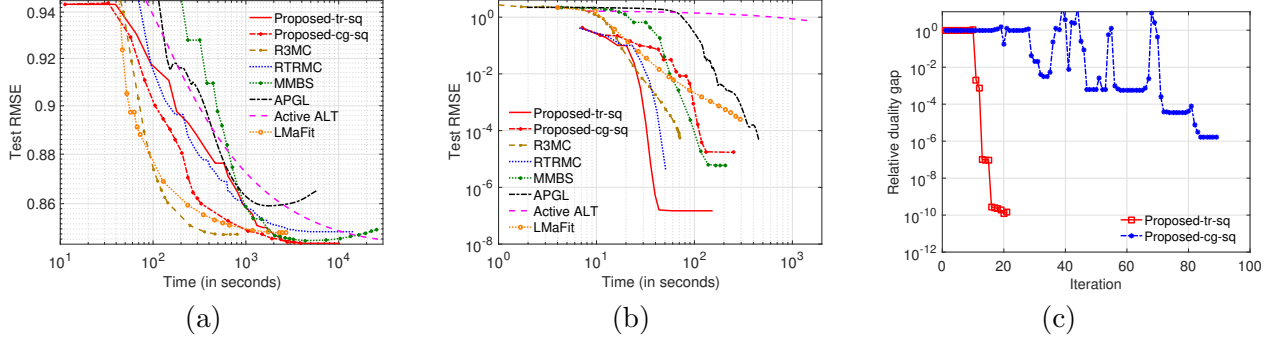


Figure 2: (a) Evolution of test RMSE on the Netflix data set (matrix completion problem). Test RMSE above the top of the y-axis are not shown. The proposed first-order and second-order algorithms, Proposed-cg-sq and Proposed-tr-sq respectively, achieve the lowest test RMSE and are computationally efficient; (b) Evolution of test RMSE on the synthetic data set. Both our methods obtain very low test RMSE; (c) Variation of the relative duality gap per iteration for our methods on the synthetic data set. It can be observed that our second-order algorithm (Proposed-tr-sq) has a better rate of convergence compared to our first-order algorithm (Proposed-cg-sq). Figure best viewed in color. Enlarged figures provided in the supplementary material.

4 Empirical Results and Discussion

In this section, we evaluate the generalization performance as well as computational efficiency of our approach against state-of-the-art in four different applications — matrix completion, robust matrix completion, Hankel matrix learning and multi-task learning. We also discuss the global convergence of our solution with respect to the convex problem (1). All our algorithms are implemented using the Manopt toolbox (Boumal et al., 2014). Implementation details, data set statistics, and additional results are provided in the supplementary material.

4.1 Matrix Completion

The following algorithms are compared for the matrix completion problem:

- APGL: An accelerated proximal gradient algorithm for nuclear norm minimization (Toh & Yun, 2010).
- Active ALT: State-of-the-art first-order nuclear norm solver based on active subspace selection (Hsieh & Olsen, 2014).
- MMBS: A fixed rank second-order nuclear norm minimization algorithm (Mishra et al., 2013).
- R3MC: A fixed-rank preconditioned non-linear conjugate gradient algorithm (Mishra & Sepulchre, 2014).
- RTRMC: A fixed-rank second-order Riemannian preconditioned algorithm on the Grassmann manifold (Boumal & Absil, 2011, 2015).
- LMaFit: A nonlinear successive over-relaxation algorithm (Wen et al., 2012).
- Proposed-cg-sq: Our conjugate gradient algorithm (Algorithm 1) with square loss (Table 1, row 1).
- Proposed-tr-sq: Our trust-region algorithm (Algorithm 1) with square loss (Table 1, row 1).

Experimental Setup. The regularization parameters are tuned to obtain the best generalization performance for all the algorithms. The optimization strategies for the competing algorithm are set to those prescribed by their authors. For instance, the line-search, continuation and truncation options are kept on for APGL. The initialization for all the algorithms is based on the first few

singular vectors of the given (incomplete) matrix (Boumal & Absil, 2015). All the algorithms are provided the same rank r (or maximum rank, in case of variable rank approaches) parameter. For synthetic and real world data sets, r is set to 5 and 10 respectively. For real world data sets, we run all the methods on ten random 80 – 20 train-test splits of the observed entries and report the root mean squared error on the test set (test RMSE) averaged over ten splits.

Synthetic data set. We choose $d = 5\,000$, $T = 500\,000$ and $r = 5$ to create a synthetic data set (with $< 1\%$ observed entries), following the procedure detailed by Boumal & Absil (2011, 2015). The number of observed entries for both training ($|\Omega|$) and testing is 15 149 850. The generalization performance of different algorithms are shown in Figure 2(b). For the same run, we plot the variation of the relative duality gap across iterations for our algorithms in Figure 2(c). It is observed that Proposed-tr-sq approach the global optima for the nuclear norm regularized problem (1) in few iterations and obtain test RMSE $\approx 2.46 \times 10^{-7}$. Our first-order algorithm, Proposed-cg-sq, also achieves lower test RMSE at much a faster rate compared to other convex approaches (APGL and Active ALT). Note that similar to RTRMC, our algorithms are able to exploit the case $d \ll T$ (rectangular matrices).

Real world data sets. We compare the algorithms on three real world data sets: Netflix (Recht & Ré, 2013), MovieLens10m (ML10m), and MovieLens20m (ML20m) data sets (MovieLens, 1997). Table A.4.1 reports the test RMSE obtained by all the algorithms. Both our algorithms obtain the best generalization results. Figure 2(a) displays the evolution of test RMSE against the training time for all the algorithms. Both Proposed-cg-sq and Proposed-tr-sq are efficient in converging to a good quality solution.

4.2 Robust Matrix Completion

We next present the results on robust matrix completion problem. We compare our algorithms (Proposed-cg-ab and Proposed-tr-ab) with state-of-the-art robust matrix completion solver RMC (Cambier & Absil, 2016). RMC is a first-order Riemannian optimization algorithm and minimizes the smooth pseudo-Huber loss function (which successively approximates absolute loss). In contrast, our methods employ the non-smooth absolute-value loss function. It should be emphasized that the non-smooth nature of absolute-value loss makes it challenging to optimize in large-scale settings. Both these loss functions are known to be robust to noise. We followed the experimental setup described in the previous section. Figure 3(a) displays the results on the Netflix data set. We observe that both our algorithms scale effortlessly on the Netflix data set and achieve generalization performance comparable to RMC. The average test RMSE obtained by Proposed-tr-ab, Proposed-cg-ab,

Table 2: Generalization performance on large-scale matrix completion data sets. We report mean result over ten random train-test split. The proposed algorithms, Proposed-tr-sq and Proposed-cg-sq, achieve the lowest test RMSE.

	Netflix	ML10m	ML20m
Proposed-tr-sq	0.8443	0.8026	0.7962
Proposed-cg-sq	0.8449	0.8026	0.7963
R3MC	0.8478	0.8070	0.7982
RTRMC	0.8489	0.8161	0.8044
APGL	0.8635	0.8283	0.8160
Active ALT	0.8463	0.8116	0.8033
MMBS	0.8499	0.8226	0.8053
LMaFit	0.8484	0.8082	0.7996

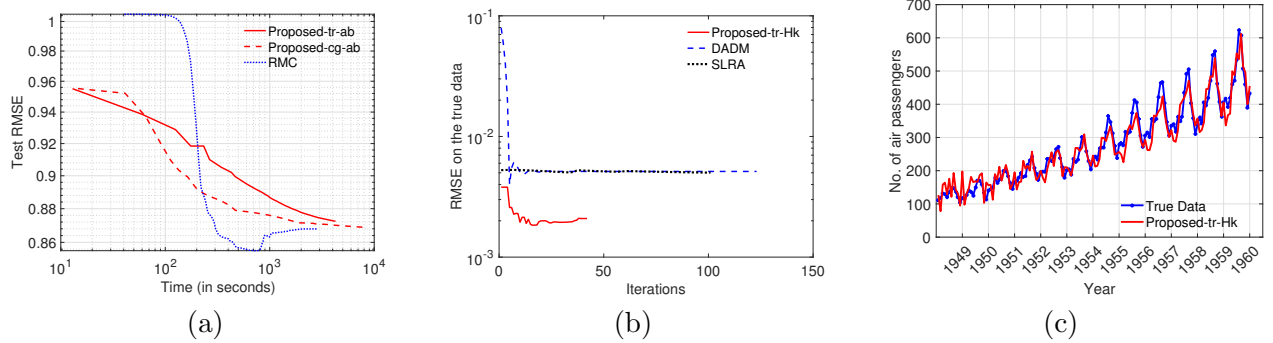


Figure 3: (a) Evolution of test RMSE of different robust matrix completion algorithms on the Netflix data set. Note that the proposed algorithms, Proposed-cg-ab (first-order) and Proposed-tr-ab (second-order), employ the non-smooth absolute-value loss function. At convergence, their generalization performance are comparable to state-of-the-art RMC algorithm, which employs smoothed pseudo-Huber loss function; (b) Performance of low rank Hankel matrix learning algorithms on the synthetic data set. Our algorithm, Proposed-tr-Hk, learns a low rank Hankel matrix with the lowest error; (c) Performance of Proposed-tr-Hk on a real world low rank Hankel matrix learning problem. Our algorithm is able to learn the monthly variations in the true data. Figure best viewed in color.

and RMC are 0.8724, 0.8690, and 0.8678 respectively.

4.3 Low-rank Hankel Matrix Learning

As discussed in Section 2.3, a Hankel matrix has the structural constraint that its anti-diagonal entries are same. Table 1 row 4 provides detailed expression for $g(\mathbf{U}\mathbf{U}^\top)$ for learning low-rank Hankel matrix.

Experimental setup. We compare our low-rank Hankel matrix learning algorithm, Proposed-tr-Hk (trust-region), with state-of-the-art solvers SLRA (Markovsky, 2014; Markovsky & Usevich, 2014) and DADM (Fazel et al., 2013). SLRA employs a variable projection method with rank constraint. On the other hand, DADM solves a trace norm regularized formulation via alternating direction methods.

We compared the algorithms on synthetic and real world data sets. The synthetic data set is generated by the procedure described by Markovsky & Usevich (2014). We learn a rank 5 Hankel matrix with $d = 1000$ and $T = 10000$. We also perform experiments on the airline passenger data set (Box & Jenkins, 1990). This is a time-series data set and contains the number of monthly passengers for twelve years. The seasonal variance in the number of monthly passengers possesses a Hankel structure. The goal here is to learn a rank 10 matrix with $d = 11$ and $T = 134$.

Results. Figure 3(b) plots the RMSE with respect to the true data on the synthetic data set. It shows that the our method learns the closest low-rank approximation of the given Hankel matrix. Figure 3(c) shows that our method is able to learn the seasonal variation in the number of passengers. The RMSE with respect to the true data obtained by SLRA, DADM and Proposed-tr-Hk are 0.0443, 0.1018, and 0.0506 respectively.

4.4 Multi-task Learning

As discussed in Section 2, problem (1) without $\mathbf{W} \in \mathcal{D}$ constraints has been employed in the mulit-task feature learning application (Argyriou et al., 2008). Existing works (Amit et al., 2007; Argyriou et al., 2008) have shown that the trace norm penalization learns the task parameters

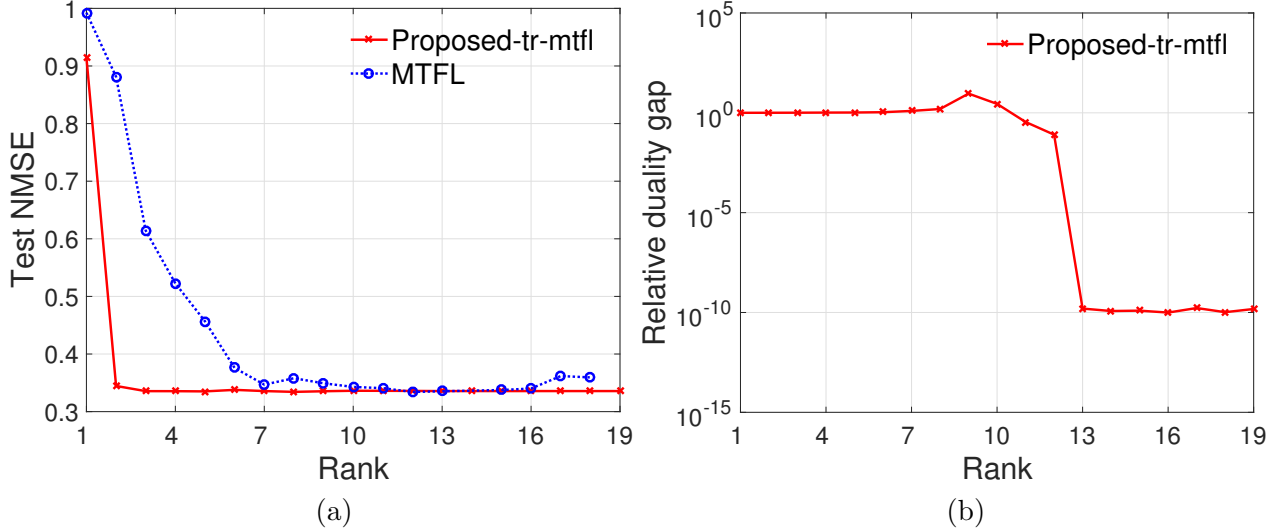


Figure 4: (a) Variation of the normalized mean squared error (NMSE) on test set with rank of the optimal solution on Parkinsons data set. Our multi-task feature learning algorithm, Proposed-tr-mt, obtains the best generalization at much lower rank compared to state-of-the-art MTFL; (b) The relative duality gap (Δ) corresponding to the optimal solutions obtained by our algorithm at different ranks. A small Δ implies that our optimal solution is also the optimal solution of the trace norm regularized formulation (1). Figure best viewed in color.

$(w_t)_{t=1}^T$ in a low-dimensional latent feature subspace. In this context, it should be noted that our approach directly learns a r dimensional latent feature space \mathbf{U} shared across all the tasks. The proposed multi-task feature learning formulation, termed as Proposed-tr-mtfl (trust-region), is a special case of (5). It follows from Lemma 3 that if r is sufficiently large, we learn a r dimensional latent subspace which is also a global solution to the trace-normalized multi-task feature learning problem (Argyriou et al., 2008). We compare the generalization performance of Proposed-tr-mtfl with the optimal solution of (1).

Experimental setup. We compare our algorithm with the MTFL algorithm (Argyriou et al., 2008). MTFL solves problem (1) without the $\mathbf{W} \in \mathcal{D}$ constraint, optimally in the multi-task feature learning setup. Optimal solution for MTFL at different ranks is obtained by tracing the solution path with respect to parameter C , whose value is varied as $\{2^{-8}, 2^{-7}, \dots, 2^{24}\}$. We vary parameter r for our algorithm to obtain different ranked solutions for a given C . The experiments are performed on two benchmark multi-task regression data sets: a) Parkinsons: we need to predict the Parkinson’s disease symptom score of 42 patients (Frank & Asuncion, 2010); b) School: we need to predict performance of all students in 139 schools. We report normalized mean square error over the test set (Argyriou et al., 2008; Zhang & Yeung, 2010).

Results. Figures 4(a)-(b) present the results on the Parkinsons data set. We observe from Figure 4(a) that our method achieves the better generalization performance at low ranks compared to MTFL. In addition, Figure 4(b) shows that we attain small duality gap when $r \geq 13$. Hence, our method optimally solves (1) at $r \geq 13$. Similar results are obtained on the School data set (details are in supplementary).

5 Conclusion

We propose a generic framework for learning low-rank matrices with structural constraints, in a large-scale setting. We pose the structured low-rank matrix learning problem as a saddle point optimization problem. The benefit of this modeling is that it decouples the low-rank and structural constraints onto separate factors. The saddle point problem is shown to lie on the Riemannian spectrahedron manifold. This enables to propose efficient Riemannian conjugate gradient and trust-region algorithms. Our algorithms scale readily on the Netflix data set even with non-smooth loss functions such as the absolute-value loss. We obtain state-of-the-art generalization performance on standard and robust matrix completion, low-rank Hankel matrix learning, and multi-task learning problems.

References

- Absil, P.-A., Mahony, R., and Sepulchre, R. *Optimization Algorithms on Matrix Manifolds*. Princeton University Press, Princeton, NJ, 2008.
- Amit, Y., Fink, M., Srebro, N., and Ullman, S. Uncovering shared structures in multiclass classification. In *International Conference on Machine Learning (ICML)*, pp. 17–24, 2007.
- Argyriou, A., Evgeniou, T., and Pontil, M. Multi-task feature learning. In *Neural Information Processing Systems conference (NIPS)*, 2006.
- Argyriou, A., Evgeniou, T., and Pontil, M. Convex multi-task feature learning. *Machine Learning*, 73:243–272, 2008.
- Barrett, R., Berry, M., Chan, T. F., Demmel, J., Donato, J., Dongarra, J., Eijkhout, V., Pozo, R., Romine, C., and der Vorst, H. Van. *Templates for the Solution of Linear Systems: Building Blocks for Iterative Methods, 2nd Edition*. SIAM, 1994.
- Bertsekas, D. *Nonlinear Programming*. Athena Scientific, 1999. URL <http://www.athenasc.com/nonlinbook.html>.
- Bonnabel, S. Stochastic gradient descent on Riemannian manifolds. *IEEE Transactions on Automatic Control*, 58(9):2217–2229, 2013.
- Bonnans, J. F. and Shapiro, A. *Perturbation Analysis of Optimization Problems*. Springer-Verlag, 2000.
- Boumal, N. and Absil, P.-A. RTRMC: A Riemannian trust-region method for low-rank matrix completion. In *Advances in Neural Information Processing Systems 24 (NIPS)*, pp. 406–414, 2011.
- Boumal, N. and Absil, P.-A. Low-rank matrix completion via preconditioned optimization on the Grassmann manifold. *Linear Algebra and its Applications*, 475:200–239, 2015.
- Boumal, N., Mishra, B., Absil, P.-A., and Sepulchre, R. Manopt: a Matlab toolbox for optimization on manifolds. *Journal of Machine Learning Research*, 15(Apr):1455–1459, 2014.
- Box, G. E. P. and Jenkins, G. *Time Series Analysis, Forecasting and Control*. Holden-Day, Incorporated, 1990.

- Boyd, S. and Vandenberghe, L. *Convex Optimization*. Cambridge University Press, 2004. URL <http://www.stanford.edu/~boyd/cvxbook/>.
- Burer, S. and Monteiro, R.D.C. A nonlinear programming algorithm for solving semidefinite programs via low-rank factorization. *Mathematical Programming*, 95(2):329–357, 2003.
- Cai, J. F., Candès, E. J., and Shen, Z. A singular value thresholding algorithm for matrix completion. *SIAM Journal on Optimization*, 20(4):1956–1982, 2010.
- Cambier, L. and Absil, P. A. Robust low-rank matrix completion by Riemannian optimization. *SIAM J. Sci. Comput.*, 38(5):S440–S460, 2016.
- Candès, E. J. and Plan, Y. Matrix completion with noise. *Proceedings of the IEEE*, 98(6):925–936, 2009.
- Candès, E. J. and Recht, B. Exact matrix completion via convex optimization. *Foundations of Computational Mathematics*, 9(6):717–772, 2009.
- Candès, E. J., Li, X., Ma, Y., and Wright, J. Robust principal component analysis? *Journal of the ACM (JACM)*, 58(3):11, 2011.
- Ciliberto, C., Mroueh, Y., Poggio, T., and Rosasco, L. Convex learning of multiple tasks and their structure. In *International Conference on Machine learning (ICML)*, 2015.
- Fazel, M., Hindi, H., and Boyd, S. P. A rank minimization heuristic with application to minimum order system approximation. In *American Control Conference*, pp. 4734–4739, 2001.
- Fazel, M., Kei, P. T., Sun, D., and Tseng, P. Hankel matrix rank minimization with applications to system identification and realization. *SIAM Journal on Matrix Analysis and Applications*, 34(3):946–977, 2013.
- Frank, A. and Asuncion, A. UCI machine learning repository, 2010. URL <http://archive.ics.uci.edu/ml>.
- Ho, C. H. and Lin, C. J. Large-scale linear support vector regression. *Journal of Machine Learning Research*, 13(1):3323–3348, 2012.
- Hsieh, C.-J. and Olsen, P. A. Nuclear norm minimization via active subspace selection. In *International Conference on Machine learning (ICML)*, 2014.
- Jawanpuria, P. and Nath, J. S. Multi-task multiple kernel learning. In *SIAM International Conference on Data Mining (SDM)*, pp. 828–83, 2011.
- Journée, M., Bach, F., Absil, P.-A., and Sepulchre, R. Low-rank optimization on the cone of positive semidefinite matrices. *SIAM Journal on Optimization*, 20(5):2327–2351, 2010.
- Kannan, R., Ishteva, M., and Park, P. Bounded matrix factorization for recommender system. *Knowledge and information systems*, 39(3):491–511, 2014.
- Markovsky, I. Recent progress on variable projection methods for structured low-rank approximation. *Signal Processing*, 96(Part B):406–419, 2014.
- Markovsky, I. and Usevich, K. Structured low-rank approximation with missing data. *SIAM Journal on Matrix Analysis and Applications*, 34(2):814–830, 2013.

- Markovsky, I. and Usevich, K. Software for weighted structured low-rank approximation. *J. Comput. Appl. Math.*, 256:278–292, 2014.
- Mishra, B. and Sepulchre, R. R3MC: A Riemannian three-factor algorithm for low-rank matrix completion. In *Proceedings of the 53rd IEEE Conference on Decision and Control (CDC)*, pp. 1137–1142, 2014.
- Mishra, B., Meyer, G., Bach, F., and Sepulchre, R. Low-rank optimization with trace norm penalty. *SIAM Journal on Optimization*, 23(4):2124–2149, 2013.
- MovieLens. MovieLens, 1997. URL <http://grouplens.org/datasets/movielens/>.
- Recht, B. and Ré, C. Parallel stochastic gradient algorithms for large-scale matrix completion. *Mathematical Programming Computation*, 5(2):201–226, 2013.
- Sato, H. and Iwai, T. A new, globally convergent Riemannian conjugate gradient method. *Optimization: A Journal of Mathematical Programming and Operations Research*, 64(4):1011–1031, 2013.
- Sato, H., Kasai, H., and Mishra, B. Riemannian stochastic variance reduced gradient. Technical report, arXiv preprint arXiv:1702.05594, 2017.
- Sion, M. On General Minimax Theorem. *Pacific Journal of Mathematics*, 1958.
- Toh, K. C. and Yun, S. An accelerated proximal gradient algorithm for nuclear norm regularized least squares problems. *Pacific Journal of Optimization*, 6(3):615–640, 2010.
- Wen, Z., Yin, W., and Zhang, Y. Solving a low-rank factorization model for matrix completion by a nonlinear successive over-relaxation algorithm. *Mathematical Programming Computation*, 4(4):333–361, 2012.
- Wright, J., Ganesh, A., Rao, S., Peng, Y., and Ma, Y. Robust principal component analysis: Exact recovery of corrupted low-rank matrices via convex optimization. In *Neural Information Processing Systems conference (NIPS)*, 2009.
- Yuan, M., Ekici, A., Lu, Z., and Monteiro, R.D.C. Dimension reduction and coefficient estimation in multivariate linear regression. *Journal of the Royal Statistical Society: Series B (Statistical Methodology)*, 69(3):329–346, 2007.
- Zhang, H., Reddi, S. J., and Sra, S. Riemannian svrg: Fast stochastic optimization on Riemannian manifolds. In *Advances in Neural Information Processing Systems (NIPS)*, pp. 4592–4600, 2016.
- Zhang, Y. and Yeung, D. Y. A convex formulation for learning task relationships in multi-task learning. In *Uncertainty in Artificial Intelligence*, 2010.

Supplementary material

Abstract

This is the supplementary material to the main paper titled ‘A Saddle Point Approach to Structured Low-rank Matrix Learning in Large-scale Applications’. Section A.1 contains the proof of Lemma 2 proposed in the main paper. Section A.2 contains the proof of Proposition 1 proposed in the main paper. Section A.3 briefly describes the Riemannian optimization framework employed in our algorithms discussed in Section 3 of the main paper. Section A.4 presents the complete experimental results and related details. The sections, equations, tables, figures and algorithms from the main paper are referred in their original numbers. The sections, equations, tables, and figures introduced in this supplementary have the numbering scheme of the form ‘A.x’.

A.1 Lemma 2 and its Proof

Lemma 2 gives the dual problem of the following primal problem with respect to variable \mathbf{W} :

$$\min_{\Theta \in \mathcal{P}^d} \sum_{t=1}^T \min_{w_t \in \mathbb{R}^d} \frac{1}{2} w_t^\top \Theta^\dagger w_t + C \sum_{i=1}^{m_t} l(y_{ti}, w_t^\top x_{ti}) \quad (\text{A.1})$$

subject to $w_t \in \text{range}(\Theta)$, $\forall t = 1, \dots, T$ and $\mathcal{A}(\mathbf{W}) = \mathbf{0}$, where $\text{range}(\Theta) = \{\Theta z : z \in \mathbb{R}^d\}$. In the following, we restate Lemma 2 from the main paper (for convenience) and prove it.

Lemma 2. *Let l_{ti}^* be the Fenchel conjugate function of the loss: $l_{ti} : \mathbb{R} \rightarrow \mathbb{R}$, $v \mapsto l(y_{ti}, v)$. The dual of (A.1) with respect to \mathbf{W} is*

$$\min_{\Theta \in \mathcal{P}^d} g(\Theta), \quad (\text{A.2})$$

where $g : \mathcal{P}^d \rightarrow \mathbb{R} : \Theta \mapsto g(\Theta)$ is the following convex function

$$\begin{aligned} g(\Theta) := & \max_{s \in \mathbb{R}^n} \sum_{t=1}^T \left(\max_{z_t \in \mathbb{R}^{m_t}} -C \sum_{i=1}^{m_t} l_{ti}^* \left(\frac{-z_{ti}}{C} \right) \right. \\ & \left. - \frac{1}{2} (\mathbf{X}_t z_t + a_t)^\top \Theta (\mathbf{X}_t z_t + a_t) \right). \end{aligned} \quad (\text{A.3})$$

Here, $a_t \in \mathbb{R}^d$ for $t = \{1, \dots, T\}$, where $[a_1, \dots, a_T] = \mathcal{A}^*(s)$ and $\mathcal{A}^* : \mathbb{R}^n \rightarrow \mathbb{R}^{d \times T}$ is the adjoint of \mathcal{A} .

Furthermore, if Θ^* be the optimal solution of (A.2) and $\{s^*, (z_t^*)_{t=1}^T\}$ be the corresponding optimal solution of (A.3), then the optimal solution $\mathbf{W}^* := [w_1^*, \dots, w_T^*]$ of (A.1) is given by $w_t^* = \Theta^*(X_t z_t^* + a_t^*)$, where $[a_1^*, \dots, a_T^*] = \mathcal{A}^*(s^*)$.

Proof. We derive the Fenchel dual function of $p : \mathbb{R}^{d \times T} \rightarrow \mathbb{R}$,

$$p(\mathbf{W}) = \sum_{t=1}^T \frac{1}{2} w_t^\top \Theta^\dagger w_t + C \sum_{i=1}^{m_t} l(y_{ti}, w_t^\top x_{ti}) \quad (\text{A.4})$$

subject to $w_t \in \text{range}(\Theta)$, $\forall t = 1, \dots, T$ and $\mathcal{A}(\mathbf{W}) = \mathbf{0}$, where $\text{range}(\Theta) = \{\Theta z : z \in \mathbb{R}^d\}$. For this purpose, we introduce the auxiliary variables $u_t \in \mathbb{R}^{m_t}$, $\forall t = 1, \dots, T$ which satisfy the constraint

$u_{ti} = w_t^\top x_{ti}$. We now introduce the dual variable $z = \{z_1, \dots, z_T\}$, $z_t \in \mathbb{R}^{m_t}$ corresponding to the constraints $u_{ti} = w_t^\top x_{ti}$, and the dual variable $s \in \mathbb{R}^n$ corresponding to the constraint $\mathcal{A}(\mathbf{W}) = \mathbf{0}$. Then the Lagrangian L of (A.4) is given as:

$$\begin{aligned} L(\mathbf{W}, u, z, s) = & -\langle s, \mathcal{A}(\mathbf{W}) \rangle + \sum_{t=1}^T \left(\frac{1}{2} w_t^\top \Theta^\dagger w_t \right. \\ & + C \sum_{i=1}^{m_t} l(y_{ti}, u_{ti}) + \sum_{i=1}^{m_t} z_{ti} (u_{ti} - w_t^\top x_{ti}) \\ & \left. + i_{\text{range}(\Theta)}(w_t) \right). \end{aligned} \quad (\text{A.5})$$

where i_H is the indicator function for set H . The dual function q of p is defined as

$$q(z, s) = \min_{\mathbf{W} \in \mathbb{R}^{d \times T}, u_t \in \mathbb{R}^{m_t} \forall t} L(\mathbf{W}, u, z, s) \quad (\text{A.6})$$

Using the definition of the conjugate function (Boyd & Vandenberghe, 2004), we get

$$\begin{aligned} \min_{u_t \in \mathbb{R}^{m_t}} & C \sum_{i=1}^{m_t} l(y_{ti}, w_t^\top x_{ti}) + \sum_{i=1}^{m_t} z_{ti} u_{ti} \\ = & -C \sum_{i=1}^{m_t} \max_{u_{ti} \in \mathbb{R}} \left(\left(-\frac{z_{ti}}{C} \right) u_{ti} - l(y_{ti}, w_t^\top x_{ti}) \right) \\ = & -C \sum_{i=1}^{m_t} l_{ti}^* \left(\frac{-z_{ti}}{C} \right), \end{aligned} \quad (\text{A.7})$$

where l_{ti}^* be the Fenchel conjugate function of the loss: $l_{ti} : \mathbb{R} \rightarrow \mathbb{R}$, $v \mapsto l(y_{ti}, v)$.

We next compute the minimizer of L with respect to w_t . From the definition of the adjoint operator, it follows that

$$\langle s, \mathcal{A}(\mathbf{W}) \rangle = \langle \mathcal{A}^*(s), \mathbf{W} \rangle$$

We define $[a_1, \dots, a_T] = \mathcal{A}^*(s)$. Then the Lagrangian L can be re-written as

$$\begin{aligned} L(\mathbf{W}, u, z, s) = & \left(\sum_{t=1}^T \sum_{i=1}^{m_t} C l(y_{ti}, u_{ti}) + z_{ti} u_{ti} \right) \\ & + \sum_{t=1}^T \left(-a_t^\top w_t + \frac{1}{2} w_t^\top \Theta^\dagger w_t + i_{\text{range}(\Theta)}(w_t) - \sum_{i=1}^{m_t} z_{ti} w_t^\top x_{ti} \right). \end{aligned}$$

The minimizer of L with respect to w_t satisfy the following conditions

$$\frac{\partial}{\partial w_t} \left(-a_t^\top w_t + \frac{1}{2} w_t^\top \Theta^\dagger w_t - \sum_{i=1}^{m_t} z_{ti} w_t^\top x_{ti} \right) = 0, \text{ and} \quad (\text{A.8})$$

$$w_t \in \text{range}(\Theta) \quad (\text{A.9})$$

which implies,

$$\Theta^\dagger w_t = \mathbf{X}_t z_t + a_t, \text{ subject to } w_t \in \text{range}(\Theta) \quad (\text{A.10})$$

Thus, the expression of the minimizer of L with respect to w_t is

$$w_t = \Theta(\mathbf{X}_t z_t + a_t).$$

Plugging the above result and (A.7) in the dual function (A.6), we obtain

$$\begin{aligned} q(z, s) = & \sum_{t=1}^T \left(-C \sum_{i=1}^{m_t} l_{ti}^* \left(\frac{-z_{ti}}{C} \right) \right. \\ & \left. - \frac{1}{2} (\mathbf{X}_t z_t + a_t)^\top \Theta (\mathbf{X}_t z_t + a_t) \right) \end{aligned}$$

□

A.2 Proof of Proposition 1

For convenience, we are reproducing the Proposition 1 from the main paper.

$$\min_{\mathbf{U} \in \mathbb{R}^{d \times r}} g(\mathbf{U}\mathbf{U}^\top), \text{ subject to } \|\mathbf{U}\|_F = 1, \quad (\text{A.11})$$

where the function $g(\mathbf{U}\mathbf{U}^\top)$ is defined as follows, *i.e.*,

$$\begin{aligned} g(\mathbf{U}\mathbf{U}^\top) := & \max_{s \in \mathbb{R}^n} \sum_{t=1}^T \max_{z_t \in \mathbb{R}^{m_t} \forall t} \left(-C \sum_{i=1}^{m_t} l_{ti}^* \left(\frac{-z_{ti}}{C} \right) \right. \\ & \left. - \frac{1}{2} \left\| \mathbf{U}^\top (X_t z_t + a_t) \right\|_F^2 \right). \end{aligned} \quad (\text{A.12})$$

Proposition 2. *Let $\hat{\mathbf{U}}$ be a feasible solution for problem (A.11). Then, the candidate solution for problem (A.2) is $\hat{\Theta} = \hat{\mathbf{U}}\hat{\mathbf{U}}^\top$. Let $\{\hat{s}, (\hat{z}_t)_{t=1}^T\}$ be the optimal solution of the convex problem (A.12) associated with the computation of $g(\hat{\mathbf{U}}\hat{\mathbf{U}}^\top)$. In addition, let σ_1 be the maximum singular of the matrix whose t^{th} column is $(X_t \hat{z}_t + \hat{a}_t)$, where $[\hat{a}_1, \dots, \hat{a}_T] = \mathcal{A}^*(\hat{s})$. The duality gap (Δ) associated with $\{\hat{\Theta}, \hat{s}, (\hat{z}_t)_{t=1}^T\}$ for problem (A.2) is given by*

$$\Delta = \frac{1}{2} \left(\sigma_1^2 - \sum_{t=1}^T \left\| \hat{\mathbf{U}}^\top (X_t \hat{z}_t + \hat{a}_t) \right\|_F^2 \right). \quad (\text{A.13})$$

Proof. Given $\hat{\Theta} = \hat{\mathbf{U}}\hat{\mathbf{U}}^\top$ as described above, the objective value of the min-max problem (A.2) is

$$\begin{aligned} g(\hat{\Theta}) = & -C \sum_{t=1}^T \sum_{i=1}^{m_t} l_{ti}^* \left(\frac{-\hat{z}_{ti}}{C} \right) \\ & - \frac{1}{2} \sum_{t=1}^T \left\langle \hat{\Theta}, (X_t \hat{z}_t + \hat{a}_t)(X_t \hat{z}_t + \hat{a}_t)^\top \right\rangle. \end{aligned} \quad (\text{A.14})$$

Using the min-max interchange (Sion, 1958), the max-min problem corresponding to (A.2) is as follows

$$\max_{s \in \mathbb{R}^n} \max_{z_t \in \mathbb{R}^{m_t} \forall t} \left(-C \sum_{t=1}^T \sum_{i=1}^{m_t} l_{ti}^* \left(\frac{-z_{ti}}{C} \right) - \frac{1}{2} B \right) \quad (\text{A.15})$$

where

$$B = \max_{\Theta \in \mathcal{P}^d} \left\langle \hat{\Theta}, \sum_{t=1}^T (X_t \hat{z}_t + \hat{a}_t)(X_t \hat{z}_t + \hat{a}_t)^\top \right\rangle. \quad (\text{A.16})$$

Note that problem (A.16) is a well studied problem in the duality theory. It is one of the definitions of the spectral norm (maximum eigenvalue of a matrix) – as the dual of the trace norm (Boyd & Vandenberghe, 2004). Its optimal value is the spectral norm of the matrix $\sum_{t=1}^T (X_t \hat{z}_t + \hat{a}_t)(X_t \hat{z}_t + \hat{a}_t)^\top$ (Boyd & Vandenberghe, 2004). Let σ_1 be the maximum singular of the matrix $E = \sum_{t=1}^T (X_t \hat{z}_t + \hat{a}_t)(X_t \hat{z}_t + \hat{a}_t)^\top$. Then the spectral norm of E is σ_1^2 . Note that the t^{th} column of E is $(X_t \hat{z}_t + \hat{a}_t)$. Putting together the above result, the objective value of the max-min problem, given $\{\hat{s}, (\hat{z}_t)_{t=1}^T\}$ is

$$G = -C \sum_{t=1}^T \sum_{i=1}^{m_t} l_{ti}^* \left(\frac{-\hat{z}_{ti}}{C} \right) - \frac{1}{2} \sigma_1^2.$$

Therefor, the duality gap (Δ) associated with $\{\hat{\Theta}, \hat{s}, (\hat{z}_t)_{t=1}^T\}$ for problem (A.2) is given by

$$\begin{aligned} \Delta &= g(\hat{\Theta}) - G \\ &= \frac{1}{2} \left(\sigma_1^2 - \sum_{t=1}^T \left\langle \hat{\Theta}, (X_t \hat{z}_t + \hat{a}_t)(X_t \hat{z}_t + \hat{a}_t)^\top \right\rangle \right) \\ &= \frac{1}{2} \left(\sigma_1^2 - \sum_{t=1}^T \left\| \hat{\mathbf{U}}^\top (X_t \hat{z}_t + \hat{a}_t) \right\|^2 \right) \end{aligned} \quad (\text{A.17})$$

The last equality is obtained by using $\hat{\Theta} = \hat{\mathbf{U}} \hat{\mathbf{U}}^\top$. □

A.3 Optimization on Spectrahedron

We are interested in the optimization problem of the form

$$\min_{\Theta \in \mathcal{P}^d} f(\Theta), \quad (\text{A.18})$$

where \mathcal{P}^d is the set of $d \times d$ positive semi-definite matrices with unit trace and $f : \mathcal{P}^d \rightarrow \mathbb{R}$ is a smooth function. A specific interest is when we seek matrices of rank r . Using the parameterization $\Theta = \mathbf{U} \mathbf{U}^\top$, the problem (A.18) is formulated as

$$\min_{\mathbf{U} \in \mathcal{S}_r^d} f(\mathbf{U} \mathbf{U}^\top), \quad (\text{A.19})$$

where $\mathcal{S}_r^d := \{\mathbf{U} \in \mathbb{R}^{d \times r} : \|\mathbf{U}\|_F = 1\}$, which is called the spectrahedron manifold (Journée et al., 2010). It should be emphasized the objective function in (A.19) is *invariant* to the post multiplication of \mathbf{U} with orthogonal matrices of size $r \times r$, i.e., $\mathbf{U} \mathbf{U}^\top = \mathbf{U} \mathbf{Q} (\mathbf{U} \mathbf{Q})^\top$ for all $\mathbf{Q} \in \mathcal{O}(r)$, which is the set of orthogonal matrices of size $r \times r$ such that $\mathbf{Q} \mathbf{Q}^\top = \mathbf{Q}^\top \mathbf{Q} = \mathbf{I}$. An implication of this observation is that the minimizers of (A.19) are no longer isolated in the matrix space, but are isolated in the quotient space, which is the set of equivalence classes $[\mathbf{U}] := \{\mathbf{U} \mathbf{Q} : \mathbf{Q} \mathbf{Q}^\top = \mathbf{Q}^\top \mathbf{Q} = \mathbf{I}\}$. Consequently, the search space is

$$\mathcal{M} := \mathcal{S}_r^d / \mathcal{O}(r). \quad (\text{A.20})$$

In other words, the optimization problem (A.19) has the structure of optimization on the *quotient* manifold, i.e.,

$$\min_{[\mathbf{U}] \in \mathcal{M}} f([\mathbf{U}]), \quad (\text{A.21})$$

but numerically, by necessity, algorithms are implemented in the matrix space \mathcal{S}_r^d , which is also called the *total space*.

Table A.1: Matrix characterization of notions on the quotient manifold $\mathcal{S}_r^d/\mathcal{O}(r)$.

Matrix representation of an element	\mathbf{U}
Total space \mathcal{S}_r^d	$\{\mathbf{U} \in \mathbb{R}^{d \times r} : \ \mathbf{U}\ _F = 1\}$
Group action	$\mathbf{U} \mapsto \mathbf{U}\mathbf{Q}$, where $\mathbf{Q} \in \mathcal{O}(r)$.
Quotient space \mathcal{M}	$\mathcal{S}_r^d/\mathcal{O}(r)$
Tangent vectors in the total space \mathcal{S}_r^d at \mathbf{U}	$\{\mathbf{Z} \in \mathbb{R}^{d \times r} : \text{trace}(\mathbf{Z}^\top \mathbf{U}) = 0\}$
Metric between the tangent vector $\xi_{\mathbf{U}}, \eta_{\mathbf{U}} \in T_{\mathbf{U}}\mathcal{S}_r^d$	$\text{trace}(\xi_{\mathbf{U}}^\top \eta_{\mathbf{U}})$
Vertical tangent vectors at \mathbf{U}	$\{\mathbf{U}\mathbf{A} : \mathbf{A} \in \mathbb{R}^{r \times r}, \mathbf{A}^\top = -\mathbf{A}\}$
Horizontal tangent vectors	$\{\xi_{\mathbf{U}} \in T_{\mathbf{U}}\mathcal{S}_r^d : \xi_{\mathbf{U}}^\top \mathbf{U} = \mathbf{U}^\top \xi_{\mathbf{U}}\}$

Below, we briefly discuss the manifold ingredients and their matrix characterizations for (A.21). Specific details of the spectrahedron manifold are discussed in (Journée et al., 2010). A general introduction to manifold optimization and numerical algorithms on manifolds are discussed in (Absil et al., 2008).

A.3.1 Tangent vector representation as horizontal lifts

Since the manifold \mathcal{M} , defined in (A.20), is an abstract space, the elements of its tangent space $T_{[\mathbf{U}]} \mathcal{M}$ at $[\mathbf{U}]$ also call for a matrix representation in the tangent space $T_{\mathbf{U}}\mathcal{S}_r^d$ that respects the equivalence relation $\mathbf{U}\mathbf{U}^\top = \mathbf{U}\mathbf{Q}(\mathbf{U}\mathbf{Q})^\top$ for all $\mathbf{Q} \in \mathcal{O}(r)$. Equivalently, the matrix representation of $T_{[\mathbf{U}]} \mathcal{M}$ should be restricted to the directions in the tangent space $T_{\mathbf{U}}\mathcal{S}_r^d$ on the total space \mathcal{S}_r^d at \mathbf{U} that do not induce a displacement along the equivalence class $[\mathbf{U}]$. In particular, we decompose $T_{\mathbf{U}}\mathcal{S}_r^d$ into complementary subspaces, the *vertical* $\mathcal{V}_{\mathbf{U}}$ and *horizontal* $\mathcal{H}_{\mathbf{U}}$ subspaces, such that $\mathcal{V}_{\mathbf{U}} \oplus \mathcal{H}_{\mathbf{U}} = T_{\mathbf{U}}\mathcal{S}_r^d$.

The vertical space $\mathcal{V}_{\mathbf{U}}$ is the tangent space of the equivalence class $[\mathbf{U}]$. On the other hand, the horizontal space $\mathcal{H}_{\mathbf{U}}$, which is any complementary subspace to $\mathcal{V}_{\mathbf{U}}$ in $T_{\mathbf{U}}\mathcal{S}_r^d$, provides a valid matrix representation of the abstract tangent space $T_{[\mathbf{U}]} \mathcal{M}$. An abstract tangent vector $\xi_{[\mathbf{U}]} \in T_{[\mathbf{U}]} \mathcal{M}$ at $[\mathbf{U}]$ has a unique element in the horizontal space $\xi_{\mathbf{U}} \in \mathcal{H}_{\mathbf{U}}$ that is called its *horizontal lift*. Our specific choice of the horizontal space is the subspace of $T_{\mathbf{U}}\mathcal{S}_r^d$ that is the *orthogonal complement* of $\mathcal{V}_{\mathbf{U}}$ in the sense of a *Riemannian metric*.

The Riemannian metric at a point on the manifold is a inner product that is defined in the tangent space. An additional requirement is that the inner product needs to be *invariant* along the equivalence classes (Absil et al., 2008, Chapter 3). One particular choice of the Riemannian metric on the total space \mathcal{S}_r^d is

$$\langle \xi_{\mathbf{U}}, \eta_{\mathbf{U}} \rangle_{\mathbf{U}} := \text{trace}(\xi_{\mathbf{U}}^\top \eta_{\mathbf{U}}), \quad (\text{A.22})$$

where $\xi_{\mathbf{U}}, \eta_{\mathbf{U}} \in T_{\mathbf{U}}\mathcal{S}_r^d$. The choice of the metric (A.22) leads to a natural choice of the metric on the quotient manifold, i.e.,

$$\langle \xi_{[\mathbf{U}]}, \eta_{[\mathbf{U}]} \rangle_{[\mathbf{U}]} := \text{trace}(\xi_{\mathbf{U}}^\top \eta_{\mathbf{U}}), \quad (\text{A.23})$$

where $\xi_{[\mathbf{U}]}$ and $\eta_{[\mathbf{U}]}$ are abstract tangent vectors in $T_{[\mathbf{U}]} \mathcal{M}$ and $\xi_{\mathbf{U}}$ and $\eta_{\mathbf{U}}$ are their horizontal lifts in the total space \mathcal{S}_r^d , respectively. Endowed with this Riemannian metric, the quotient manifold

\mathcal{M} is called a *Riemannian* quotient manifold of \mathcal{S}_r^d .

Table A.1 summarizes the concrete matrix operations involved in computing horizontal vectors.

Additionally, starting from an arbitrary matrix (an element in the ambient dimension $\mathbb{R}^{d \times r}$), two linear projections are needed: the first projection $\Psi_{\mathbf{U}}$ is onto the tangent space $T_{\mathbf{U}}\mathcal{S}_r^d$ of the total space, while the second projection $\Pi_{\mathbf{U}}$ is onto the horizontal subspace $\mathcal{H}_{\mathbf{U}}$.

Given a matrix $\mathbf{Z} \in \mathbb{R}^{d \times r}$, the projection operator $\Psi_{\mathbf{U}} : \mathbb{R}^{d \times r} \rightarrow T_{\mathbf{U}}\mathcal{S}_r^d : \mathbf{Z} \mapsto \Psi_{\mathbf{U}}(\mathbf{Z})$ on the tangent space is defined as

$$\Psi_{\mathbf{U}}(\mathbf{Z}) = \mathbf{Z} - \text{trace}(\mathbf{Z}^\top \mathbf{U})\mathbf{U}. \quad (\text{A.24})$$

Given a tangent vector $\xi_{\mathbf{U}} \in T_{\mathbf{U}}\mathcal{S}_r^d$, the projection operator $\Pi_{\mathbf{U}} : T_{\mathbf{U}}\mathcal{S}_r^d \rightarrow \mathcal{H}_{\mathbf{U}} : \xi_{\mathbf{U}} \mapsto \Pi_{\mathbf{U}}(\xi_{\mathbf{U}})$ on the horizontal space is defined as

$$\Pi_{\mathbf{U}}(\xi_{\mathbf{U}}) = \xi_{\mathbf{U}} - \mathbf{U}\mathbf{\Lambda}, \quad (\text{A.25})$$

where $\mathbf{\Lambda}$ is the solution to the *Lyapunov* equation

$$(\mathbf{U}^\top \mathbf{U})\mathbf{\Lambda} + \mathbf{\Lambda}(\mathbf{U}^\top \mathbf{U}) = \mathbf{U}^\top \xi_{\mathbf{U}} - \xi_{\mathbf{U}}^\top \mathbf{U}.$$

A.3.2 Retractions from Horizontal Space to Manifold

An iterative optimization algorithm involves computing a search direction (*e.g.*, the gradient direction) and then moving in that direction. The default option on a Riemannian manifold is to move along geodesics, leading to the definition of the exponential map. Because the calculation of the exponential map can be computationally demanding, it is customary in the context of manifold optimization to relax the constraint of moving along geodesics. The exponential map is then relaxed to a *retraction* operation, which is any map $R_{\mathbf{U}} : \mathcal{H}_{\mathbf{U}} \rightarrow \mathcal{S}_r^d : \xi_{\mathbf{U}} \mapsto R_{\mathbf{U}}(\xi_{\mathbf{U}})$ that locally approximates the exponential map on the manifold (Absil et al., 2008, Definition 4.1.1). On the spectrahedron manifold, a natural retraction of choice is

$$R_{\mathbf{U}}(\xi_{\mathbf{U}}) := (\mathbf{U} + \xi_{\mathbf{U}}) / \|\mathbf{U} + \xi_{\mathbf{U}}\|_F, \quad (\text{A.26})$$

where $\|\cdot\|_F$ is the Frobenius norm and $\xi_{\mathbf{U}}$ is a search direction on the horizontal space $\mathcal{H}_{\mathbf{U}}$.

An update on the spectrahedron manifold is, thus, based on the update formula $\mathbf{U}_+ = R_{\mathbf{U}}(\xi_{\mathbf{U}})$.

A.3.3 Riemannian Gradient and Hessian Computations

The choice of the invariant metric (A.22) and the horizontal space turns the quotient manifold \mathcal{M} into a *Riemannian submersion* of $(\mathcal{S}_r^d, \langle \cdot, \cdot \rangle)$. As shown by Absil et al. (2008), this special construction allows for a convenient matrix characterization of the gradient and the Hessian of a function on the abstract manifold \mathcal{M} .

The matrix characterization of the Riemannian gradient is

$$\text{grad}_{\mathbf{U}} f = \Psi_{\mathbf{U}}(\nabla_{\mathbf{U}} f), \quad (\text{A.27})$$

where $\nabla_{\mathbf{U}} f$ is the Euclidean gradient of the objective function f and $\Psi_{\mathbf{U}}$ is the tangent space projector (A.24).

An iterative algorithm that exploits second-order information usually requires the Hessian applied along a search direction. This is captured by the Riemannian Hessian operator Hess , whose matrix characterization, given a search direction $\xi_{\mathbf{U}} \in \mathcal{H}_{\mathbf{U}}$, is

$$\begin{aligned} \text{Hess}_{\mathbf{U}}[\xi_{\mathbf{U}}] = \Pi_{\mathbf{U}} \Big(& \text{D}\nabla f[\xi_{\mathbf{U}}] - \text{trace}((\nabla_{\mathbf{U}} f)^\top \mathbf{U})\xi_{\mathbf{U}} \\ & - \text{trace}((\nabla_{\mathbf{U}} f)^\top \xi_{\mathbf{U}} + (\text{D}\nabla f[\xi_{\mathbf{U}}])^\top \mathbf{U})\mathbf{U} \Big), \end{aligned} \quad (\text{A.28})$$

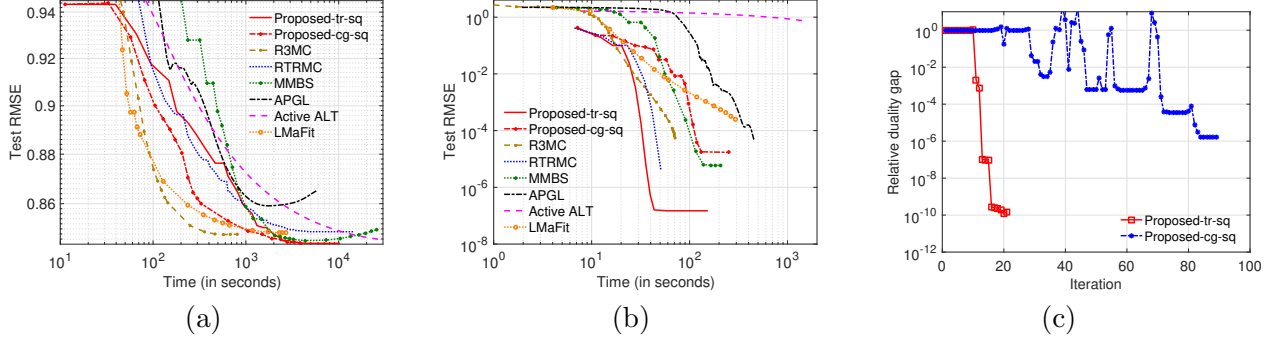


Figure A.1: (a) Evolution of test RMSE on the Netflix data set (matrix completion problem). Test RMSE above the top of the y-axis are not shown. The proposed first-order and second-order algorithms, Proposed-cg-sq and Proposed-tr-sq respectively, achieve the lowest test RMSE and are computationally efficient; (b) Evolution of test RMSE on the synthetic data set. Both our methods obtain very low test RMSE; (c) Variation of the relative duality gap per iteration for our methods on the synthetic data set. It can be observed that our second-order algorithm (Proposed-tr-sq) has a better rate of convergence compared to our first-order algorithm (Proposed-cg-sq). Figure best viewed in color.

where $D\nabla f[\xi_{\mathbf{U}}]$ is the directional derivative of the Euclidean gradient $\nabla_{\mathbf{U}} f$ along $\xi_{\mathbf{U}}$ and $\Pi_{\mathbf{U}}$ is the horizontal space projector (A.25).

Finally, the formulas in (A.27) and (A.28) that the Riemannian gradient and Hessian operations require only the expressions of the standard (Euclidean) gradient of the objective function f and the directional derivative of this gradient (along a given search direction) to be supplied.

A.4 Empirical Results and Discussion

In this section, we discuss our results in four different applications — matrix completion, robust matrix completion, Hankel matrix learning and multi-task learning. We compare the generalization performance as well as computational efficiency of our approach against state-of-the-art in each of the above applications. We also discuss the global convergence of our solution with respect to the convex problem (1). All our methods were implemented using the Manopt toolbox (Boumal et al., 2014).

A.4.1 Matrix Completion

The following algorithms are compared for the matrix completion problem:

- APGL: An accelerated proximal gradient approach for nuclear norm regularization with square loss function (Toh & Yun, 2010).
- Active ALT: State-of-the-art first-order nuclear norm solver based on active subspace selection (Hsieh & Olsen, 2014).
- MMBS: A second-order fixed rank nuclear norm minimization algorithm (Mishra et al., 2013). It employs an efficient factorization of the matrix \mathbf{W} which renders the trace norm regularizer differentiable in the primal formulation.
- R3MC: A non-linear conjugate gradient based approach for fixed rank matrix completion (Mishra & Sepulchre, 2014). It employs a Riemannian preconditioning technique, customized for the square loss function.

- RTRMC: It models fixed rank matrix completion problems with square loss on the Grassmann manifold and solves it via a second order preconditioned Riemannian trust-region method (Boumal & Absil, 2011, 2015).
- LMaFit: A nonlinear successive over-relaxation based approach for low rank matrix completion with square loss (Wen et al., 2012).
- Proposed-cg-sq: Our method with conjugate gradients (Algorithm 1) and the square loss (Table 1, row 1 in the main paper).
- Proposed-tr-sq: Our method with trust-regions (Algorithm 1) and the square loss (Table 1, row 1 in the main paper).

Experimental Setup. The regularization parameters were tuned to obtain the best generalization performance for all the algorithms. The optimization strategies for the competing algorithm were set to those prescribed by their authors. For instance, line-search, continuation and truncation were kept on for APGL. The initialization was based on the first few singular vectors of the given (incomplete) matrix (Boumal & Absil, 2015). All the algorithms are provided the same rank (or maximum rank in case of variable rank approaches) parameter. For synthetic data sets, it was set to 5 and for real world data sets, it was set to 10. For real world data sets, we ran all the methods on ten random 80 – 20 train-test splits of the observed entries and report the root mean squared error on the test set (test RMSE) averaged over ten splits. The test RMSE results are reported after the algorithms have converged or have reached maximum number of iterations (`maxIter`). For first-order methods, `maxIter` is set to 500 for the Netflix data set and 200 for other smaller data sets. For second-order methods, `maxIter` is set to 100 for the Netflix data set and 60 for other smaller data sets.

Synthetic data set. We choose $d = 5\,000$, $T = 500\,000$ and $r = 5$ to create a synthetic data set (with $< 1\%$ observed entries), following the procedure detailed by Boumal & Absil (2011, 2015). The number of observed entries for both training ($|\Omega|$) and testing was 15 149 850. The generalization performance of different methods is shown in Figure A.1(a). For the same run, we also plot the variation of the relative duality gap across iterations for our methods in figure A.1(b). It can be observed that Proposed-tr-sq approach the global optima for the nuclear norm regularized problem (1) in very few iterations and obtain test RMSE $\approx 2.46 \times 10^{-7}$. Our first order algorithm, Proposed-cg-sq, also achieves lower test RMSE at much faster rate compared to other convex approaches — APGL and Active ALT. Note that similar to RTRMC, our methods are able to exploit the condition that $d \ll T$ (rectangular matrices).

Real world data set. We tested the methods on three real world data sets: Netflix (Recht & Ré, 2013), MovieLens10m (ML10m) and MovieLens20m (ML20m) (MovieLens, 1997). Their statistics are given in Table A.4.1. Following Boumal & Absil (2015), we center the data around the mean of the training data. Table A.4.1 reports the test RMSE obtained by all the approaches on these three data sets. Both our methods obtain the best generalization results. Figure A.1(a) displays the evolution of test RMSE for all the methods. Proposed-cg-sq and Proposed-tr-sq are highly efficient in obtaining lower test RMSE compared to other convex approaches (APGL and Active ALT).

Table A.2: Data set statistics for the matrix completion application.

	d	T	$ \Omega $
Netflix	17 770	480 189	100 198 805
ML10m	10 677	71 567	10 000 054
ML20m	26 744	138 493	20 000 263

Table A.3: Generalization performance of various algorithms on the matrix completion problem. The table reports mean result along with the standard deviation over ten random train-test split. The proposed algorithms achieve the lowest test RMSE.

	Netfix	MovieLens10m	MovieLens20m
Proposed	0.8443 ± 0.0001	0.8026 ± 0.0005	0.7962 ± 0.0003
Proposed-cg	0.8449 ± 0.0003	0.8026 ± 0.0005	0.7963 ± 0.0003
R3MC	0.8478 ± 0.0001	0.8070 ± 0.0004	0.7982 ± 0.0003
RTRMC	0.8489 ± 0.0001	0.8161 ± 0.0004	0.8044 ± 0.0005
APGL	0.8635 ± 0.0009	0.8283 ± 0.0009	0.8160 ± 0.0013
Active ALT	0.8463 ± 0.0005	0.8116 ± 0.0012	0.8033 ± 0.0008
MMBS	0.8499 ± 0.0002	0.8226 ± 0.0015	0.8053 ± 0.0008
LMaFit	0.8484 ± 0.0001	0.8082 ± 0.0005	0.7996 ± 0.0003

A.4.2 Robust Matrix Completion

We next present the results for robust matrix completion problem. We compare our first- and second-order algorithms, Proposed-cg-ab and Proposed-tr-ab respectively, with state-of-the-art robust matrix completion solver RMC (Cambier & Absil, 2016). RMC is a first order Riemannian optimization algorithm and minimizes the smooth pseudo-Huber loss function (which successively approximates absolute loss). In contrast, our methods employ the non-smooth absolute loss function. Both these loss functions are known to be robust to noise but optimizing the non-smooth absolute loss function is more challenging, especially in large scale setting. We followed the experimental setup described in previous section. Figure A.2 displays the results on the Netflix data set. We observe that both the proposed methods scale effortlessly on the Netflix data set and achieve generalization performance comparable to RMC. The average test RMSE obtained by Proposed-tr-ab, Proposed-cg-ab, and RMC are 0.8724 ± 0.0002 , 0.8690 ± 0.0002 , and 0.8678 ± 0.0002 respectively.

A.4.3 Hankel Matrix Learning

As discussed in Section 2 of the main paper, a Hankel matrix has the structural constraint that its anti-diagonal entries are same. Table 1 row 4 in the main paper provides the expression for $g(\mathbf{U}\mathbf{U}^\top)$ and a corresponding solver for learning low-rank Hankel matrix.

Experimental setup. We compare our low-rank Hankel matrix learning algorithm, Proposed-tr-Hk (second order algorithm), with state-of-the-art solvers SLRA (Markovsky, 2014; Markovsky & Usevich, 2014) and DADM (Fazel et al., 2013). SLRA employs a variable projection method to optimizes the square loss function with rank constraint and learn low rank Hankel matrix. On the other hand, DADM solves a trace norm regularized formulation via alternating direction methods.

We compared the methods on synthetic and real world data sets. The synthetic data set was generated by the procedure described by Markovsky & Usevich (2014). The procedure generated a vector y of length 10999 and added a Gaussian noise to y to get the vector \hat{y} . The goal is to learn a rank 5 Hankel matrix (with $d = 1000$ and $T = 10000$) corresponding to vector y but all the three algorithms are provided the vector \hat{y} . We also perform experiments on the airline passenger data set (Box & Jenkins, 1990). This is a time-series data set and contains the number of monthly passengers for twelve years. The seasonal variance in the number of monthly passengers possesses the Hankel structure. We learn a rank 10 Hankel matrix (with $d = 11$ and $T = 134$) corresponding to 144 data readings (y). As in the case of synthetic data, we added Gaussian noise to y to simulate the realistic setting that the vector given to the algorithms has noise. We measure the RMSE with

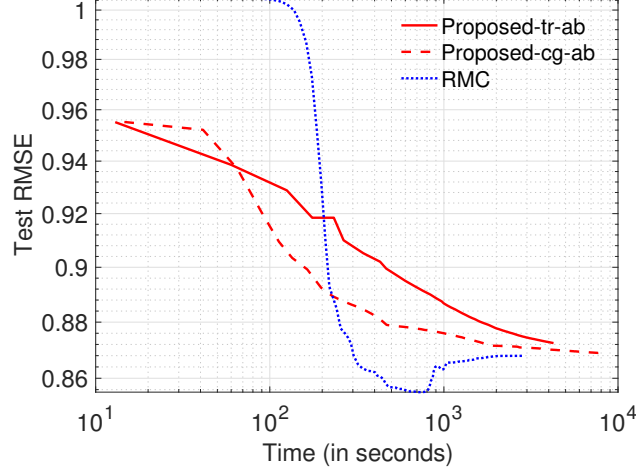


Figure A.2: Evolution of test RMSE of different robust matrix completion algorithms on the Netflix data set. Note that the proposed algorithms, Proposed-cg-ab (first-order) and Proposed-tr-ab (second-order), employ the non-smooth absolute-value loss function. At convergence, their generalization performance are comparable to state-of-the-art RMC algorithm, which employs smoothed pseudo-Huber loss function. Figure best viewed in color.

respect to the true data (y) as a measure of performance.

Results. Figure A.3(a) plots the RMSE with respect to the true data on the synthetic data set. It shows that our method learns the closest low-rank approximation of the given Hankel matrix. Figure A.3(b) compares the evolution of RMSE on true data with time for our algorithms, Proposed-cg-Hk (first-order) and Proposed-tr-Hk (second-order), and DADM on the synthetic data set. Note that both these methods are implemented in Matlab. SLRA is not compared in this experiment since it is completely implemented in C/C++ and is much faster compared to DADM and our algorithms. Figure A.3(c) shows that our method is able to model the seasonal variation in the number of airlines passengers quite accurately. The RMSE with respect to the true data obtained by SLRA, DADM and Proposed-tr-Hk are 0.0443, 0.1018, and 0.0506 respectively.

A.4.4 Multi-task Learning

As discussed in Section 2 of the main paper, problem (1), without $\mathbf{W} \in \mathcal{D}$ constraint, has been employed in the multi-task feature learning application (Argyriou et al., 2008). Existing works (Amit et al., 2007; Argyriou et al., 2008) have shown that the trace norm penalization learns the task parameters $(w_t)_{t=1}^T$ in a low-dimensional latent feature subspace. In this context, it should be noted that our framework directly learns a r dimensional latent feature space \mathbf{U} shared across all the tasks. The proposed multi-task feature learning formulation, termed as Proposed-tr-mtfl (second order algorithm), is a special case of (5). It follows from Lemma 3 (in the main paper) that if r is sufficiently large, we learn a feature space *equivalent* to the one learned by the trace-norm regularized multi-task formulation (Argyriou et al., 2008). In this multi-task feature learning setting, we compare the generalization performance of the proposed rank restricted solution of (1) against the optimal solution of (1).

Experimental setup. We compare against the MTFM algorithm (Argyriou et al., 2008) which optimally solves problem (1), without the $\mathbf{W} \in \mathcal{D}$ constraint, in multi-task setup. Optimal solution for MTFM at different ranks is obtained by tracing the solution path with respect to parameter C , which was varied in the set $\{2^{-8}, 2^{-7}, \dots, 2^{24}\}$. If multiple C values have the same rank solution,

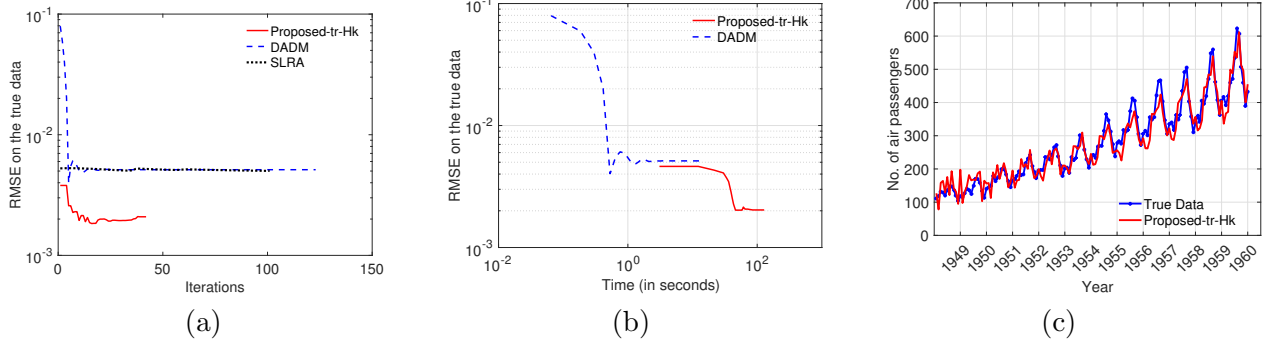


Figure A.3: (a) Performance of low rank Hankel matrix learning algorithms on the synthetic data set. Our algorithm, Proposed-tr-Hk, learns a low rank Hankel matrix with the lowest error; (b) Evolution of RMSE on true data with time for Proposed-tr-Hk (second-order), Proposed-cg-Hk (first-order) and DADM on the synthetic Hankel data set. (c) Performance of Proposed-tr-Hk on a real world low rank Hankel matrix learning problem. Our algorithm is able to learn the monthly variations in the true data. Figure best viewed in color.

C with best generalization performance on test set is chosen for that rank. Let C^* be the value of C at which the best generalization performance over test set was observed for MTF. We varied the rank r for our method to obtain different ranked solutions with $C = C^*$. The experiments were performed on two benchmark multi-task regression data sets:

- Parkinsons: We need to predict the Parkinson's disease symptom score of 42 patients (Frank & Asuncion, 2010). Each patient is described using 19 bio-medical features. The data set has a total of 5,875 readings from all the patients.
- School: The data consists of 15,362 students from 139 schools (Argyriou et al., 2008). The aim is to predict the performance of each student given their description and earlier record. Overall, each student data has 28 features. Predicting the performance of students belonging to one school is considered as one task.

We report normalized mean square error over the test set (Argyriou et al., 2008; Zhang & Yeung, 2010) for both the methods.

Results. Figure A.4(a)-(d) present the results on the Parkinsons and School data sets. We can observe from Figures A.4(a) and A.4(c) that our method, Proposed-tr-mtl, achieves the best generalization at much lower rank compared to MTF. In addition, Figures A.4(b) and A.4(d) shows that we attain a very low relative duality gap when the give rank r is large enough. Hence, for Parkinsons and School data sets, our method optimally solves (1) with $r \geq 13$ and $r \geq 5$ respectively.

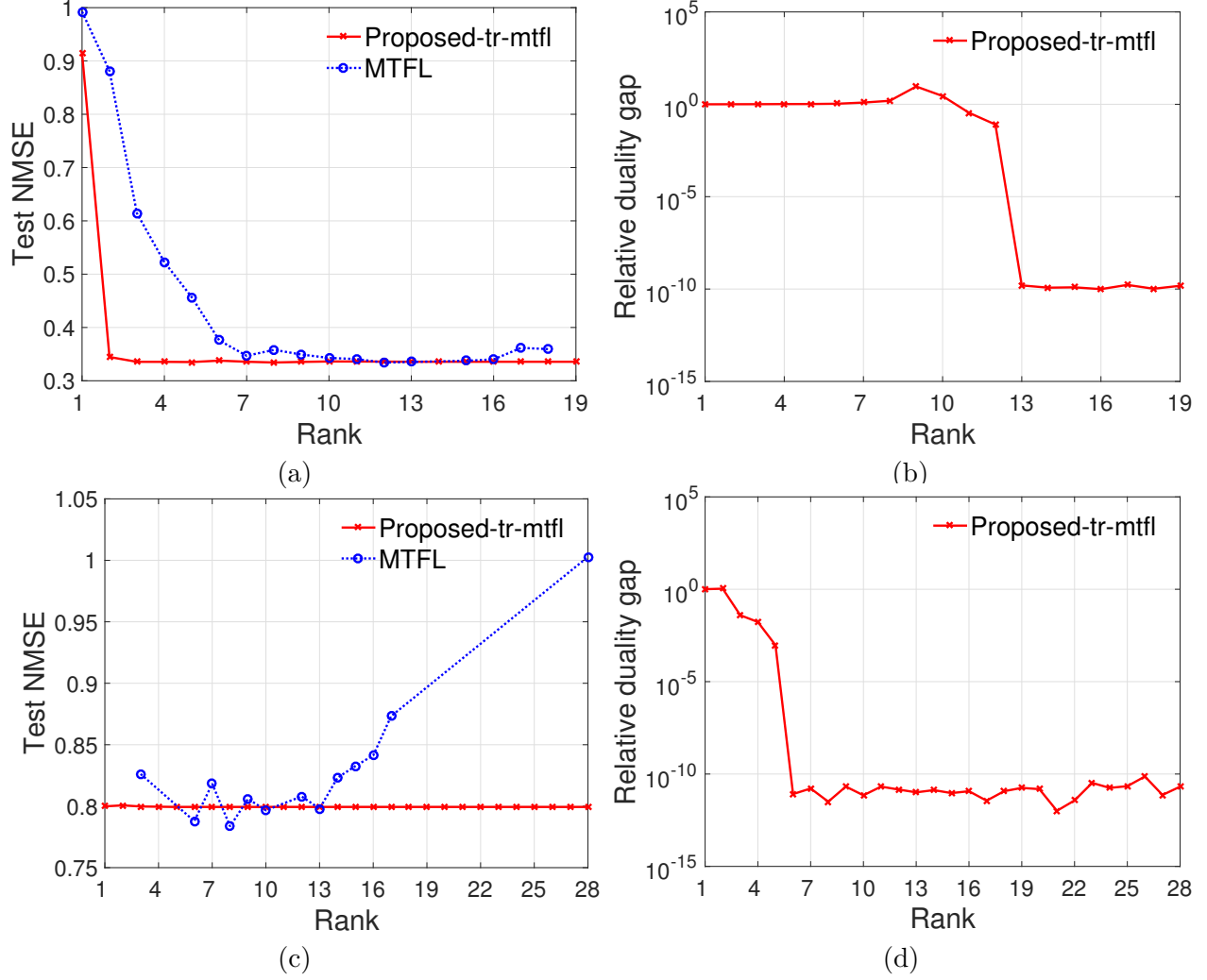


Figure A.4: (a) & (c) Variation of normalized mean squared error (NMSE) as the rank of the optimal solution changes on Parkinsons and School data sets respectively. Our multi-task feature learning method, Proposed-tr-mt, obtains best generalization at much lower rank compared to state-of-the-art MTFL algorithm (Argyriou et al., 2008); (b) & (d) The relative duality gap (Δ) corresponding to the optimal solutions obtained by our method at different ranks. A small Δ implies that our optimal solution is also the optimal solution of the trace norm regularized formulation (1). Figure best viewed in color.